Dear William,

Thank you for your time taken in your detailed and mostly positive review of the manuscript. Original comments are given in bold, which are responded to point-by-point in regular font.

General comments

This paper covers two topics, the description of a simple climate model and calculation of observationally-constrained climate sensitivity. This may be doing too much in one paper. The question of climate sensitivity is long-running and of high importance, so if the authors believe they have new insight into this it would deserve its own paper with a title that reflects this and probably not in a model development journal. Conversely if the climate sensitivity calculations are intended more as an illustration of the FAIR model then much of the detail is overkill. My review will be more focussed on the model development aspects of the paper.

Again, thank you for the time spent in reviewing the manuscript. We appreciate the point that the second part of the paper which focuses on the application of FAIR to constrain climate sensitivity may be additional detail over and above the description of the model. However, we believe it is important to show how FAIR can be useful to the climate modelling community by demonstrating its application to well-understood scenarios (the RCPs). In fact, reviewers for a paper based on this model have asked for this evidence. Since ECS and TCR must be supplied to the model, and a constraint must be applied to ensure that each combination of model parameters results in plausible output (the constraining process), it is not much of a stretch to use these results to show which input parameters of ECS and TCR result in plausible output, and provides additional confidence that the model is providing sensible results.

The FAIR model has the potential for being a very useful tool that could be widely used. Therefore the authors need to take care that it is constructed in such a way as to be generally useful and not just for RCP scenarios. For instance it should be set up to be able to take in CO2-only emissions rather than having to subtract the non-CO2 effects from RCP8.5. The paper needs to be clear as to whether this is a model that is suitable for use by the wider community yet.

Thank you for this positive comment. It is possible to run FAIR with CO_2 emissions only, where forcing from non-CO_2 agents can be specified optionally. For the TCRE assessment we now do this. As the CO_2-only treatment has already been described in Millar et al. (2017), we do not focus on this particular implementation in the present paper.

We claim that FAIR is useful for a wide range of scenarios other than the RCPs and has been designed to evaluate a wide range of emissions commitment scenarios. As the RCPs are familiar to many and span a wide range of future projections, we use them in this paper to evaluate the performance of FAIR.

For a few of the forcing agents (e.g. aircraft, land use) there is a convoluted methodology to recreate the original activity data from the RCP emissions. A tool like this should be designed to take activity data as its basic input. It is fine for this paper if the authors have recreated the activity data from the RCP in this instance to test the model, but if the FAIR tool were to be used in an aircraft or land use study it doesn't make sense to have to generate NOx or CO2 emissions from the activity data so that FAIR can then invert them to get back to the original activity data.

Thank you for this important suggestion. We agree that starting from the base activity data would be more useful in order to compare impacts. However, the model is designed to be as simple as possible, and where possible to use only the 39-species emissions data appearing in the RCPs. We argue that our simple treatment of land use forcing satisfies this simple treatment while still producing a plausible time series of ERF (noting the uncertainties in land use ERF are so wide that not even the sign of the forcing is known with confidence). See also responses below and our response to the other reviewer on this point.

For the RCP scenarios, aircraft activity data does not appear to be easily available, so we do not have any data on which to train the model to. We therefore specify the (time-varying) fraction of total NOx emissions that are due to aviation as a proxy for contrail forcing. This can be calculated from the RCP databases for RCP scenarios and is included as an option in the model where the user can use a specified RCP aviation NOx fraction (or provide their own). We argue that this is an improvement over MAGICC, which does not include contrail forcing (up to 0.5 W m^{-2} in RCP8.5 at the 95% level). Including aircraft activity data would be a valuable future improvement.

It is entirely inappropriate to use the AR5 ozone and aerosol ERF time series to back out the response coefficients by linear regression. These time series were generated by a few models (it may only have been GISS) that ran forward to generate ERFs. These time series were intended to illustrate the evolution of the ERFs, not as the last word. These are not the time series that were used to force any of the CMIP5 GCMs, nor the forcings diagnosed from CMIP5 (apart maybe from GISS). Hence the ability or not to recreate the AR5 time series using FAIR is meaningless since none of the GCMs used these. Even if these time series had been more rigorously generated it is not sensible to use linear regression to derive the response coefficients as the covariances are so large. I suggest using Stevenson et al. 2013 and Aerocom to derive response coefficients. Whichever method is used, the coefficients need to be listed in tables.

This is another important point. FAIR v1.1 was designed initially to convert as best as possible raw emissions data into an ERF time series that is used to calculate temperature change for assessing a wide range of global emissions scenarios. The AR5 Annex II time series was used to correlate RCP emissions. Obviously, many forcing and emissions components do not follow linear or other simple analytical relationships, but where possible we had determined relationships that approximately track the AR5 historical ERF time series for each forcing component.

Following your comments we have implemented the ozone forcing treatment from Stevenson et al. (2013), direct aerosol forcing treatment from Aerocom (Myhre et al., 2013a), and a representation of the aerosol indirect effect from the simplified model of Ghan et al. (2013), informed by the aerosol indirect effect treatment in Stevens (2015). These changes result in different future forcing and temperature time series to v1.1, in particular a warming of around 0.5 K in RCP8.5 in 2100 compared to the old treatment owing to the increase in tropospheric ozone and (decrease in negative) aerosol forcing in the new relationships. We feel that these changes are substantial enough to warrant an increment of the model version number, so the model version in this paper is now v1.2.

Since our modified aerosol treatment is quite similar to the model of Stevens (2015) (although with more predictor variables), we remove the Stevens aerosol relationship from the sensitivity analysis in section 5.

Specific comments

Page 2, line 14: Ocean sinks will become less effective too. Is this accounted for in FAIR?

Thank you for pointing this out – this is actually a small typo, and should read “land and ocean carbon sinks”.

Page 2, lines 27-30: IPCC merely used the carbon cycle responses from Joos et al. 2013 rather than constructing anything new. The Joos et al. responses were in turn taken from fits to C4MIP so would have included any feedbacks for biospheric uptake and temperature inherent in C4MIP models.

We agree that the original statement was misleading, which was meant to imply that the Joos relationship as it is used in AR5 does not include any carbon or temperature feedbacks because all calculations are performed against a background concentration of 389 ppm. As you correctly suggest the original relationships in Joos et al. do include state-dependent feedbacks. We have changed “with no feedbacks assumed for biospheric carbon uptake

or temperature" to "where time constants were taken from a multi-model intercomparison of full- and intermediate-complexity earth system models (Joos et al., 2013) with no feedbacks assumed for biospheric carbon uptake or temperature".

Page 3, line 7: Replace "validated" with "calibrated"

We agree this is more appropriate terminology. Manuscript updated.

Page 3, line 11: It is not quite clear what "expected to be smoothed out in the global mean." Is trying to say. Obviously the global mean is an average of the regional variations by definition.

On reflection this sentence is superfluous and has been removed. We tried to highlight that we acknowledge that trying to account for a forcing mechanism in one global mean number may hide substantial localised variability, but this is implied from the zero-dimensional model described.

Page 4, equation 1: State that Ri are masses in kg.

Resolved in revised manuscript.

Page 5, equation 4: State that Ct are molar mixing ratios. Equation is missing a factor δ_t.

δ_t is 1 (at least in this model version) so was omitted but has now been added in for completeness. C_t has been explained.

Page 5, lines 3-5: The natural emissions in fig 2 look very unrealistic. What do MAGICC natural emissions look like? Do they have a different way of addressing this?

Originally, MAGICC natural emissions (for e.g. methane) are estimated by balancing the budget for the change in concentration, minus the contribution from anthropogenic emissions from the following relationship (see Meinshausen et al. (2011a) and the MAGICC Wiki page). The exact details do not appear to be straightforward.

We initially estimated natural emissions by adjusting them to approximate the observed concentration time series over the RCP historical timeframe. However we have now taken a more accurate approach and formally backed out natural emissions by taking the difference in observed concentrations, accounting for atmospheric sources and sinks, and emissions, to obtain the natural contribution over the historical period. The future natural emissions are held fixed at their 2005 values. Figure 2 in the manuscript has been updated.

Page 5, lines 19-25: The methane lifetime is a function of methane concentration and this dependence is not difficult to implement, see eg MAGICC description or IPCC

TAR 4.2.1.1. For increasing emissions the concentrations increase more rapidly than for a constant lifetime. This probably explains the discrepancy in the methane for RCP8.5 in fig 4(b).

We agree with the reviewer on this point, and we actually implemented a variable methane lifetime from Holmes et al. (2013) originally in the development process. However there are several reasons why we did not proceed in the final version:

1. The future emissions scenarios are uncertain, and a discrepancy of 5% with MAGICC for 2100 in RCP8.5 is not critical compared to the 25% error in methane forcing between Etminan et al. (2016) and Myhre et al. (1998), the latter of which we believe is used in MAGICC. Also using a sophisticated methane lifetime relationship such as that in Holmes et al. (2013) results in a deviation from MAGICC as large (in the other direction) as using a fixed lifetime for RCP8.5 in 2100.

2. There is no guarantee that the relationships that hold for small departures from present-day concentrations would apply to the more than $2\times$ increase in methane concentrations projected in MAGICC for 2100; see for example the diversity in methane lifetime and equilibrium concentrations for the NOx attribution experiment in Stevenson et al. (2013, Table 7)

3. In the context of this work, some level of natural emissions have to be assumed post-2005 to balance the historical time series up to 2005, and it is not clear what treatment has been applied in the RCPs post-2005. To illustrate this we have experimented by implementing a simple methane feedback lifetime (where a 1% change in concentrations results in a 0.32% change in lifetime, the best estimate given in AR5), starting with an unrealistically short lifetime of 7 years in the pre-industrial in order to approximate 9.3 years in 2005, with no dependence on other effects (Holmes et al. (2013) show that methane concentration is the most important single effect on methane lifetime, even if overestimated). This results in the time series of natural balancing emissions in fig. 1 below for RCP8.5. Natural emissions of methane become negative before 2100 even under this low estimate of methane lifetime which is probably implausible; for more realistic pre-industrial and present day lifetimes, the natural emissions become more negative.

We don't rule out returning to the question of a varying methane lifetime in future model versions, and agree with the reviewer that this would be more satisfying. In our experience so far however, the additional complexity is not only unjustified but leads to unlikely methane concentrations being returned.

Page 6, section 2.1.3: This section needs an explanation of how to avoid double counting as the CO_2 emissions are often based on the total fuel consumed rather than

specifically how much is fully oxidised all the way to CO_2.

We take the same approach as in MAGICC and do not assume that the CO_2 emissions inventories include oxidation of fossil sources of CH_4 (Meinshausen et al. (2011a, eq. A1)). The RCP scenarios, derived from MAGICC originally and also used for evaluation of FAIR, are based on total fuel consumption as detailed in Meinshausen et al. (2011b), using data from Marland et al. (2008), which in turn uses the method of Marland and Rotty (1984). Although not explicitly stated, following the argument in Marland and Rotty (1984) implies that natural gas that is not burned, incompletely combusted, or used for ammonia production accumulates as methane in the atmosphere.

Thus a molecule emitted as methane and not combusted is counted as methane until it is oxidised to CO_2. The atmospheric sink provides a mechanism for removal of methane. We have added the following sentence:

"As atmospheric methane concentrations are reduced by exponential decay in eq. (5), this prevents against (approximately) double-counting an emitted fossil-fuel CH_4 molecule as both CH_4 and CO_2 after it has been oxidised."

Page 6, line 14: Myhre et al. 2013b did not show that ERF agrees with RF, rather they found that there had not been sufficient research to determine whether the ERF was different to RF. As the authors are well aware the PDRMIP project amongst others has compared RF and ERF more recently.

This sentence has been changed:

"Although Etminan et al. (2016) calculate RF, Myhre et al. (2013b) concluded that over the industrial era there was not sufficient evidence to state that ERF was significantly different from RF for these three gases, and ERF is taken to equal RF, although with a doubled uncertainty range."

Page 7, section 2.2.2: Use "well-mixed greenhouse gases" to exclude ozone.

Included in revised version.

Page 7, section 2.3.3: This linear regression is not an appropriate way to derive the response coefficients since the historical emissions strongly co-vary. Deriving a negative correspondence with NMVOC is not merely an interesting detail, it is physically wrong and so undermines the whole procedure. This must also mean that some or all of the other coefficients are overestimated to compensate. While this method may give acceptable agreement for the RCP scenarios in fig 5(e) it would give incorrect predictions when applied to more idealised scenarios e.g. if the FAIR tool were used to assess the climate impact of biomass stoves. There are sufficient data in Stevenson

et al. 2013 to be able to derive more physically credible coefficients. The coefficients need to be provided in a table and compared with other studies.

Following these comments we have re-introduced the Stevenson et al. (2013) relationships, and they are tabulated in table 4 in the manuscript. To be consistent with Stevenson et al. (2013) and the natural emissions from Skeie et al. (2011), recognising that anthropogenic emissions in 1750 were not zero, we implement a different coefficient set for RCP scenarios before 1850.

Page 8, section 2.2.5. The AR5 value assumed stratospheric water vapour added 15% of the Myhre et al. 1998 methane RF. It would add a lower percentage of the Eminan et al. ERF.

You are correct in that the upward revision from Etminan et al. (2016) for methane forcing would cause an upward increase in stratospheric water vapour forcing. This was detectable in fig. 5g. In v1.2, the model has been updated so that the scaling relationship depends on the forcing option used. We change the default value to 12% of the methane forcing reflecting that the ratio of Myhre et al. (1998) to Etminan et al. (2016) methane forcing is approximately 4/5. The actual scaling factor can be over-ridden by the user. The impact is actually fairly small at about 0.02 W m^{-2} in the present day.

Page 8, section 2.2.6: It is dangerous to build in this back calculation of aircraft activity into a tool. It is much safer to use activity data as the input. If the authors have chosen to back activity data out from RCP datasets for the purpose of this paper that's fine, but it shouldn't be hidden within the tool.

We appreciate your concern with the treatment of contrail radiative forcing. To our knowledge, the aircraft activity figures going into the RCP datasets are not readily available so could not be used for this particular instance. Additionally, the contribution to total emissions from aviation are not available for most species; NOx is one of the few where this is available. In any case, the aviation NOx fraction is specified by the user as a time series or constant, and the RCP values can be pre-loaded from within FAIR. We agree that an option to specify aviation activity would be a useful future development.

Page 8, section 2.2.7: As with ozone, linear regression is not an appropriate way to derive the response coefficients. Using speciated RFari forcing from AR5 and Aerocom to divide up the total ERFari+aci is a more transparent method. The coefficients need to be provided in a table and compared with other studies.

We agree that the old treatment may have been deficient so have updated the treatment of aerosol forcing for v1.2. Aerocom only includes the direct aerosol effect so we need a separate treatment of the indirect effect. For this we use a curve fit to the model in Ghan et al. (2013) which depends logarithmically on emissions of SOx and OC+BC. For this we

have borrowed the functional dependence of aerosol forcing on SOx emissions from Stevens (2015). This is detailed in the re-written section 2.2.7 and in the supplementary material.

Page 9, section 2.2.9: Again, it is dangerous to build in this back calculation of land use activity into a tool. It is much safer to use activity data as the input. If the authors have chosen to back activity data out from RCP datasets for the purpose of this paper that's fine, but it shouldn't be hidden within the tool. The forcing is missing a minus sign.

The missing minus sign has been included. Thank you for spotting this omission.

We wanted to make FAIR simple, and as far as possible able to derive forcing and temperature from a single RCP-style emissions dataset. For a long time during the model development, land use was supplied externally along with solar and volcanic forcing. This was slightly unsatisfactory as land use is an anthropogenic forcing. It was noticed that land use ERF in the AR5 Annex II time series actually scaled fairly well with cumulative land-use CO_2 emissions, for the reasons given in the manuscript (total deforestation since pre-industrial is linked in some way to the total amount of carbon lost to the atmosphere). Furthermore, in the future, the shapes of RCP land use forcing time series in MAGICC and FAIR are very similar, suggesting that land use CO_2 emissions are an important component of land use forcing in MAGICC. Our treatment is therefore no worse than in MAGICC, and probably simpler.

Requiring activity data for land use changes (from e.g. the gridded LUH dataset) would add significant complexity to the model for a small and uncertain forcing (see also response to other reviewer). However, like other suggestions, it would be a welcome development and could be implemented in a future version.

Page 11, section 3.3: Note the +/- 20% uncertainty in the CO2 ERF reflect uncertainty in our best estimate of the CO_2 forcing, not how it is implemented in the climate models. The actual CO2 ERF "seen" by individual GCMs may lie outside this range.

The 20% uncertainty applies to the 5–95% range around 3.71 W m^{-2}, so 10% of values going into the FULL ensemble lie outside of this range.

We should also be clear on the treatment; the Etminan et al. (2016) CO_2 forcing calculated by the model, from changes in GHG concentrations, is scaled to ensure that it equals the user-specified $F_{2\times}$ to ensure consistency between forcing and temperature change. A note at the end of section 2.2.1 has been added to explain this. In reality the user-specified value of $F_{2\times}$ actually makes very little difference to the temperature change (section 5), but affects the impact of non-CO_2 forcing on temperature as a low $F_{2\times}$ requires less non-CO_2 forcing to achieve the same unit temperature change.

Page 12, section 4.1: It is plausible that there may be an anti-correlation between

a models F2x and its climate sensitivity (in K/(W/m2)). Is this accounted for in this study? Defining ECS and TCS in terms of F2x rather than in K/(W/m2) might hide some of the model variation in F2x.

No correlation was assumed between ECS and $F_{2\times}$ in the FULL ensemble. Analysing the NROY ensemble also does not indicate any preference for high or low values of $F_{2\times}$. This is indicated in fig. 2 in this response.

Furthermore, we quickly investigated the relationship between ECS and $F_{2\times}$ from the CMIP5 results reported in Forster et al. (2013, Table 1), which shows there does not appear to be any correlation (fig. 3; this response).

Page 13, line number 15 (actually the first line!): Given that the FAIR parameters were derived from the historical GHG concentrations, it doesn't seem much of a test that it can reproduce them.

You are correct in that for methane and nitrous oxide, the comparisons to MAGICC6 can be made arbitrarily good by changing the natural emissions, and indeed have been in this updated model version (fig. 2 in paper), so a direct comparison over the historical period may not be relevant. The same could probably be argued for CFC12-eq and HFC134-eq, although natural emissions are only included for a few species and are not tuned to match concentrations except in the pre-industrial equilibrium case. However, concentration plots can demonstrate to potential users that the model is doing what is expected. Concentrations could also be used as an additional observational constraint in the CO_2 case, although we do not do that formally here as it can be seen in fig. 4a that the uncertainty around the present-day value is small in the NROY ensemble.

In the future simulations, concentration plots are useful to determine how FAIR differs from MAGICC under the simpler model setup in FAIR. It can be demonstrated the the impact of using a constant lifetime and constant natural emissions for methane and nitrous oxide is actually quite small for the RCP scenarios.

Page 13, line number 18 (3rd line): How can MAGICC reproduce the kinks in CO2, but FAIR can't?

The CO_2 time series that we compare to for pre-2005 is from observations. It is our understanding that MAGICC used prescribed GHG concentrations prior to 2005 and emissions after this date. The historical emissions time series supplied in the RCPs are from Marland et al. (2008). By this observation we were not originally correct to *assert* that MAGICC could replicate the historical concentration time series (we don't know if it can or cannot). This has been changed in the revised version. Following a suggestion from the other reviewer we have plotted the historical CO_2 as an inset so the differences are easier to see.

The behaviour of CO_2 concentrations in the future between FAIR and MAGICC when forced with the same post-2005 emissions (fig. 4a; manuscript) shows that the carbon cycles in both models actually behave very similarly over the range of RCP scenarios in the default case. It has previously been demonstrated that MAGICC and FAIR can both be set up to emulate different carbon cycle models (see Millar et al. (2017); Meinshausen et al. (2011a)).

In reality, it is likely that there is significant inter-annual variability in the exchange between land, ocean and atmosphere that affect atmospheric CO_2 concentrations on yearly timescales (a recent example being the strong El Niño of 2016-17). By its design, FAIR will not capture these small deviations with four time constants. The more appropriate test is whether it can capture the long term trend between pre-industrial and present-day. Although not used formally as a constraint, CO_2 concentrations in the best estimates for the RCPs range between 403.4 to 408.4 ppm for 2017 in the temperature-constrained ensemble, in line with observations.

Page 13, line number 28: The authors recognise the problems with a fixed methane lifetime. It is not difficult to implement this to rectify this errors.

As previously discussed, using a variable methane lifetime results in implausible methane concentrations using the RCP time series. A time-varying methane lifetime would be desirable to implement, but we feel that this is not compatible with the RCP emissions data.

Page 13, section 4.3, lines 13-14: It's not surprising the linear regression reproduces the time series it was fit to. The future ERFs need to be compared to Stevenson et al. 2013, not MAGICC.

This has now been done in v1.2 of the model.

Page 13, line 15. It is not surprising that the model can reproduce the AR5 stratospheric ozone ERF as FAIR uses exactly the same formula as AR5 (scaling with EESC).

This is by design, as the model was originally intended to emulate AR5 where there was no evidence to suggest an updated treatment (as for methane ERF). Added "as it follows the same functional relationship as AR5".

Page 13, line 17. The reason FAIR overestimates the AR5 stratospheric water vapour value is because it scales up the Etminan et al. methane forcing which is 25% larger than the Myhre et al. 1998 forcing.

This has now been updated because of the inconsistency pointed out between taking 15% of the AR5 methane forcing and 15% of the new Etminan et al. (2016) methane forcing. The resulting time series as expected is similar to AR5.

Page 15, section 4.5: Since the methane forcing is 25% stronger in FAIR, presumably the TCR has to be lower to compensate. Does this explain the lower future projections?

As you may be aware, several of the author team are involved in the IPCC Special Report on 1.5°C and this was a question that was considered. We found that the median TCR was 4% lower with the Etminan et al. (2016) relationship. It is a contributing factor, but not the only one. Changing the aerosol and tropospheric ozone relationships have in fact had a bigger impact on the TCR estimates (increase of 8% between v1.1 and v1.2).

Bottom of page 15, top of page 16: I don't understand this complicated method for calculating the TCRE to CO2-alone. Surely FAIR can be forced with just CO2 emissions and will output the temperature? If this is a CO2- alone calculation why does equation 22 account for the effect of non-co2 temperature changes?

We agree that this was originally too complex and had been re-run in CO_2 only mode with much of the old description in this section deleted. Figure 9 has been updated. The TCRE does not change much, although the all-forcing (red) curve is quite a lot higher than previously, a result of an upward revision of the future non-CO_2 forcing.

Page 18, section 5.2: This section needs to be expanded to discuss the difference between relative sensitivities in terms of F2x and absolute sensitivities in terms of K/(W/m2). If F2x is lower then the absolute sensitivity must be higher and hence the larger response when including the non-CO2 forcings.

This behaviour of higher temperatures for the same forcing under a lower F2x has now been explained using the energy budget framework in eq. 21.

Page 19, line numbered 18: I didn't understand why with a smaller (magnitude) present day aerosol forcing the 2100 temperatures are higher. Surely smaller aerosol forcing means lower TCR/ECS?

It is actually the future evolution in aerosol ERF that affects 2100 temperature change rather than the present day aerosol forcing, which has more of a bearing on ECS and TCR. As a low present day aerosol forcing also implies a low future aerosol forcing, and the full impact of ECS and TCR on temperature change has not been realised by 2100, a low aerosol forcing implies greater temperature change over this timeframe. This is further evidenced by the switch to a new aerosol relationship which has a lower 2100 aerosol forcing than in the previous version.

Tables 5–7 (now 7–9) in the manuscript have been updated with the new values.

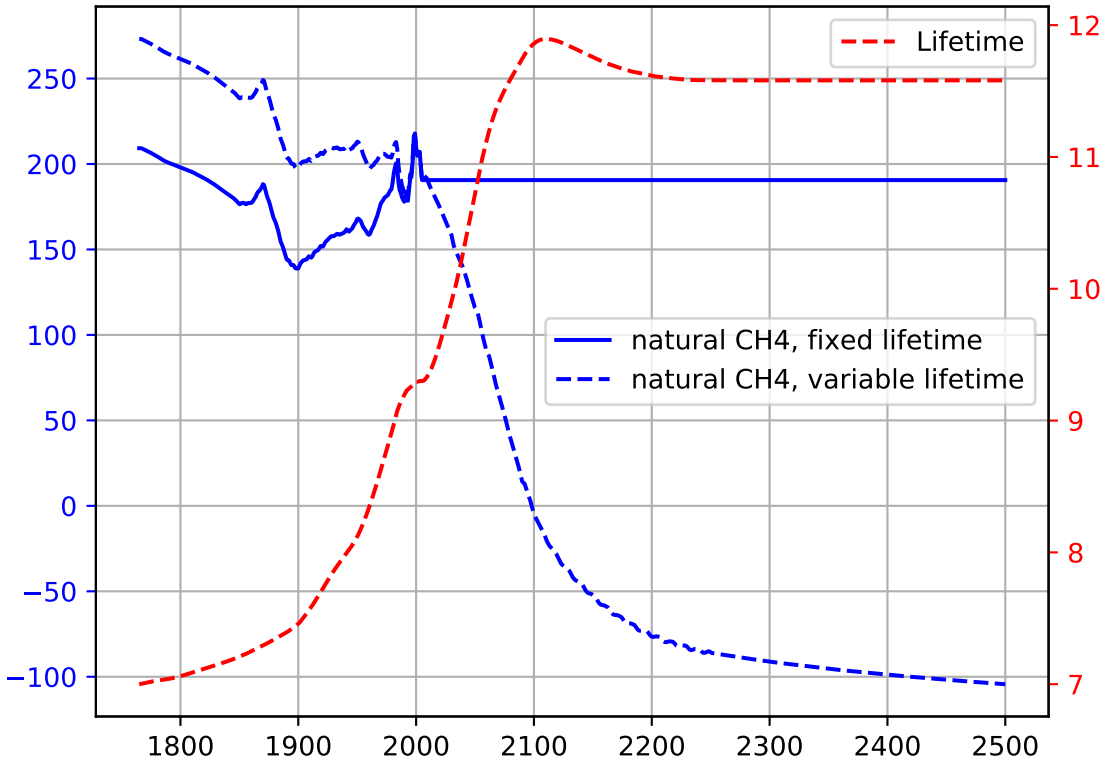

Figure 1: Effect on natural methane emissions for fixed and varying methane lifetime for RCP8.5.

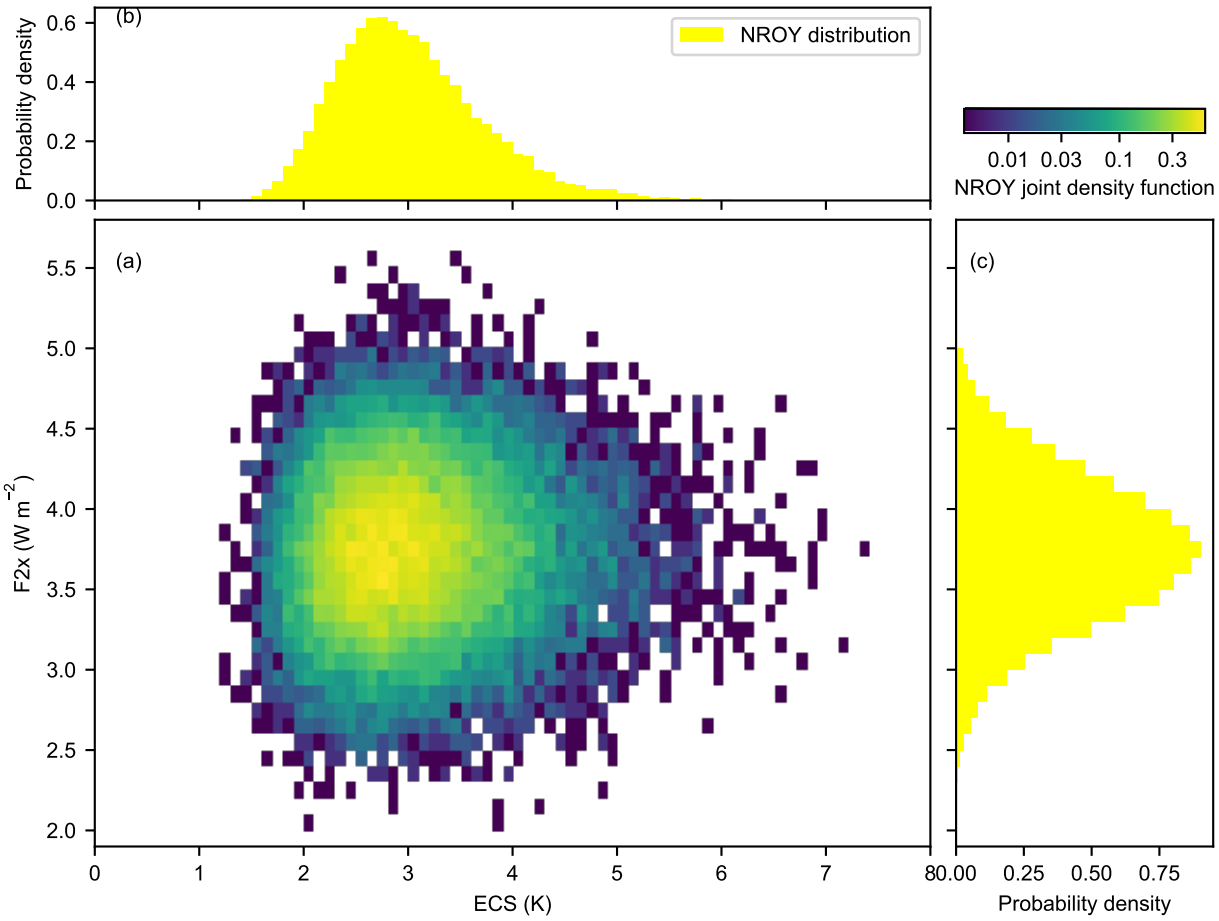

Figure 2: Joint and marginal histograms of ECS and $F_{2\times}$ in the NROY ensemble (after temperature constraint).

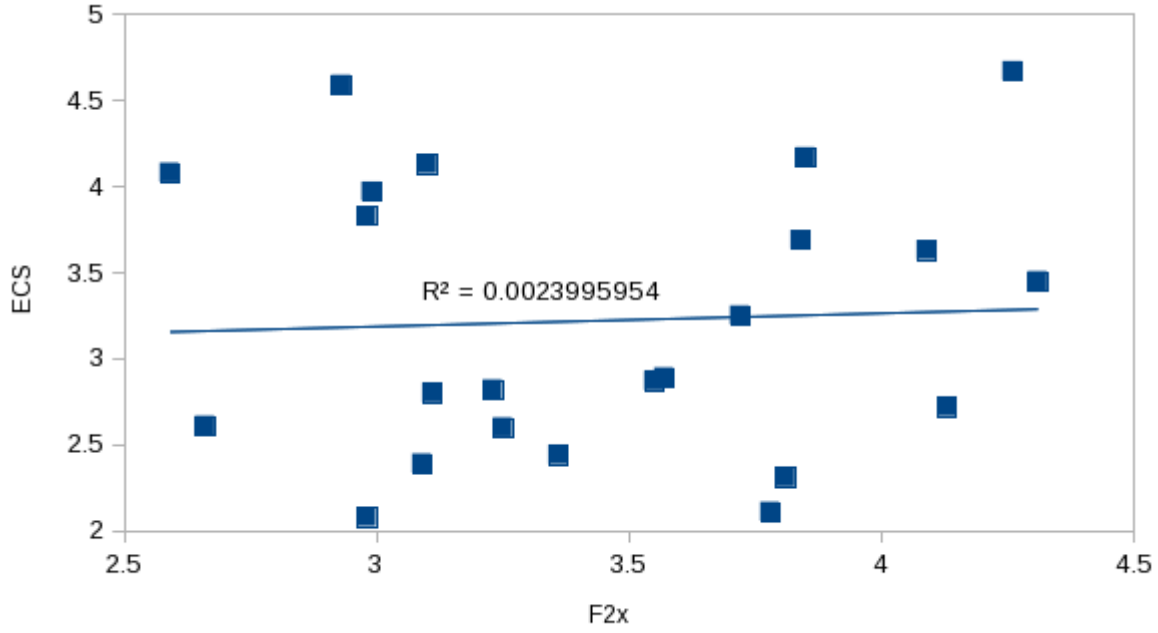

Figure 3: Scatter plot of ECS and $F_{2\times}$ for CMIP5 models in Forster et al. (2013, Table 1).

References

Etminan, M., Myhre, G., Highwood, E. J., and Shine, K. P. (2016). Radiative forcing of carbon dioxide, methane, and nitrous oxide: A significant revision of the methane radiative forcing. *Geophys. Res. Lett.*, 43(24):12,614–12,623. 2016GL071930.

Forster, P. M., Andrews, T., Good, P., Gregory, J. M., Jackson, L. S., and Zelinka, M. (2013). Evaluating adjusted forcing and model spread for historical and future scenarios in the cmip5 generation of climate models. *J. Geophys. Res.-Atmos.*, 118(3):1139–1150.

Ghan, S. J., Smith, S. J., Wang, M., Zhang, K., Pringle, K., Carslaw, K., Pierce, J., Bauer, S., and Adams, P. (2013). A simple model of global aerosol indirect effects. *J. Geophys. Res.-Atmos.*, 118(12):6688–6707.

Holmes, C. D., Prather, M. J., Søvde, O. A., and Myhre, G. (2013). Future methane, hydroxyl, and their uncertainties: key climate and emission parameters for future predictions. *Atmos. Chem. Phys.*, 13(1):285–302.

Joos, F., Roth, R., Fuglestvedt, J., Peters, G., Enting, I., von Bloh, W., Brovkin, V., Burke, E., Eby, M., Edwards, N., Friedrich, T., Frölicher, T. L., Halloran, P. R., Holden, P. B., Jones, C., Kleinen, T., Mackenzie, F. T., Matsumoto, K., Meinshausen, M., Plattner, G.-K., Reisinger, A., Segschneider, J., Shaffer, G., Steinacher, M., Strassmann, K., Tanaka, K., Timmermann, A., and Weaver, A. J. (2013). Carbon dioxide and climate impulse response functions for the computation of greenhouse gas metrics: a multi-model analysis. *Atmos. Chem. Phys.*, 13(5):2793–2825.

Marland, G., Boden, T., and Andres, R. (2008). Global, Regional, and National Fossil Fuel CO_2Emissions. `http://dx.doi.org/10.3334/CDIAC/00001_V2010`. Accessed 12 February 2018.

Marland, G. and Rotty, R. (1984). Carbon dioxide emissions from fossil fuels: a procedure for estimation and results for 1950–1982. *Tellus B*, 36B(4):232–261.

Meinshausen, M., Raper, S., and Wigley, T. (2011a). Emulating coupled atmosphere-ocean and carbon cycle models with a simpler model, MAGICC6 – Part 1: Model description and calibration. *Atmos. Chem. Phys.*, 11:1417–1456.

Meinshausen, M., Smith, S., Calvin, K., Daniel, J., Kainuma, M., Lamarque, J.-F., Matsumoto, K., Montzka, S., Raper, S., Riahi, K., Thomson, A., Velders, G., and van Vuuren, D. (2011b). The RCP Greenhouse Gas Concentrations and their Extension from 1765 to 2300. *Climatic Change*.

Millar, R. J., Nicholls, Z. R., Friedlingstein, P., and Allen, M. R. (2017). A modified impulse-response representation of the global near-surface air temperature and atmospheric concentration response to carbon dioxide emissions. *Atmos. Chem. Phys.*, 2017:7213–7228.

Myhre, G., Highwood, E. J., Shine, K. P., and Stordal, F. (1998). New estimates of radiative forcing due to well mixed greenhouse gases. *Geophys. Res. Lett.*, 25(14):2715–2718.

Myhre, G., Samset, B. H., Schulz, M., Balkanski, Y., Bauer, S., Berntsen, T. K., Bian, H., Bellouin, N., Chin, M., Diehl, T., Easter, R. C., Feichter, J., Ghan, S. J., Hauglustaine, D., Iversen, T., Kinne, S., Kirkevåg, A., Lamarque, J.-F., Lin, G., Liu, X., Lund, M. T., Luo, G., Ma, X., van Noije, T., Penner, J. E., Rasch, P. J., Ruiz, A., Seland, Ø., Skeie, R. B., Stier, P., Takemura, T., Tsigaridis, K., Wang, P., Wang, Z., Xu, L., Yu, H., Yu, F., Yoon, J.-H., Zhang, K., Zhang, H., and Zhou, C. (2013a). Radiative forcing of the direct aerosol effect from AeroCom Phase II simulations. *Atmos. Chem. Phys.*, 13(4):1853–1877.

Myhre, G., Shindell, D., Bréon, F.-M., Collins, W., Fuglestvedt, J., Huang, J., Koch, D., Lamarque, J.-F., Lee, D., Mendoza, B., Nakajima, T., Robock, A., Stephens, G., Takemura, T., and Zhang, H. (2013b). Anthropogenic and natural radiative forcing. In Stocker, T., Qin, D., Plattner, G.-K., Tignor, M., Allen, S., Boschung, J., Nauels, A., Xia, Y., Bex, V., and Midgley, P., editors, *Climate Change 2013: The Physical Science Basis. Contribution of Working Group I to the Fifth Assessment Report of the Intergovernmental Panel on Climate Change*, pages 659–740. Cambridge University Press, Cambridge, United Kingdom and New York, NY, USA.

Skeie, R., Berntsen, T., Myhre, G., Tanaka, K., Kvalevåg, M., and Hoyle, C. (2011). Anthropogenic radiative forcing time series from pre-industrial times until 2010. *Atmospheric Chemistry and Physics*, 11(22):11827–11857.

Stevens, B. (2015). Rethinking the lower bound on aerosol radiative forcing. *J. Climate*, 28(12):4794–4819.

Stevenson, D. S., Young, P. J., Naik, V., Lamarque, J.-F., Shindell, D. T., Voulgarakis, A., Skeie, R. B., Dalsoren, S. B., Myhre, G., Berntsen, T. K., Folberth, G. A., Rumbold, S. T., Collins, W. J., MacKenzie, I. A., Doherty, R. M., Zeng, G., van Noije, T. P. C., Strunk, A., Bergmann, D., Cameron-Smith, P., Plummer, D. A., Strode, S. A., Horowitz, L., Lee, Y. H., Szopa, S., Sudo, K., Nagashima, T., Josse, B., Cionni, I., Righi, M., Eyring, V., Conley, A., Bowman, K. W., Wild, O., and Archibald, A. (2013). Tropospheric ozone changes, radiative forcing and attribution to emissions in the Atmospheric Chemistry and Climate Model Intercomparison Project (ACCMIP). *Atmos. Chem. Phys.*, 13(6):3063–3085.

Dear Brian,

Thank you for your time spent in reviewing this manuscript and the useful comments you provided. Original comments are given in bold, which are responded to point-by-point in regular font.

General comments

Overall the paper is a useful, relatively clear explanation of the FAIR 1.1 model, and its difference from FAIR 1.0, with a useful short summary of the FAIR 1.0 model. The paper also describes how model parameters are estimated by comparing outcomes to the observed temperature record, and then uses the derived parameter ranges to project future radiative forcing, concentrations, and global mean temperature change under the RCPs. This section serves to document, and exercise, the version of the model that incorporates uncertainty.

Thank you for your largely positive comments overall. In addition to incorporating uncertainty there are several processes that convert emissions of non-CO_2 species to radiative forcing, which is a development from FAIR v1.0.

I have a few general comments followed by a number of more specific ones. First, the overall philosophy of the model could use better highlighting. It appears that choice about design of the various model elements are guided by the desire to represent modeling approaches and parameter values presented in AR5. This is not always clear, and since other approaches are possible, it makes it a little confusing in spots why some choices were made. An early, clear statement of the approach and its rationale would be useful.

We agree that this could have been made clearer. In the introduction we now state:

"The model philosophy in FAIR is to represent these processes as simply as possible, and to be able to emulate the ERF time series in AR5 given input emissions. FAIR is written in Python and open source."

Also, we have taken this opportunity to rewrite some of the other paragraphs in the introduction to improve readability and conciseness.

Also, as noted below, some aspects of the model are insufficiently described. Also, it would be useful to more clearly indicate when new approaches to modeling specific species are being used, and when these are borrowed from existing simple models (MAGICC or others). It would be useful, for example, to provide a summary of simi-

larities/differences between FAIR and the MAGICC model, since MAGICC serves as a key point of reference for FAIR and for the evaluation of results.

We have strived to make the treatment of each process a little clearer. We highlight in section 2.2 where a process is borrowed from MAGICC or elsewhere; where this is not stated, it has been derived by the authors.

Many of the processes in MAGICC (e.g. the carbon cycle) are not easy to summarise in a simple table, and some are not known to the authors (one example being the assumptions of natural emissions used in MAGICC), so we have not included this comparison. In further work we will investigate the different responses between the models in more detail.

Last, the paper seems to downplay the difference between projected warming with the FAIR model and warming according to Rogelj et al as reported in AR5. But this amounts to a full degree difference in the 2081-2100 mean under RCP8.5, which is a very substantial difference. This difference in results should be more clearly indicated (quantified in the abstract), and its reasons (difference in ECS/TCR and historical radiative forcing) pointed out more prominently. Related to this, the sensitivity of ECS/TCR (and warming) to prior distributions seems also downplayed, by indicating they are of equal importance as other factors (temperature record, eg) which have a substantially smaller quantitative effect on results. This particular factor should be identified as especially important.

Thank you for this important comment. Following the comments from the other reviewer, some of the assumptions made for the scientific components of the model have now been improved, particularly for tropospheric ozone and aerosols. The consequences are that the constrained distributions of ECS and TCR are a little higher than previously and we don't see the full degree difference in RCP8.5 any more (it is about 0.5K).

The last sentence of the abstract has been modified:

"The range of temperature projections under RCP8.5 for 2081–2100 in the constrained FAIR model ensemble is lower than the emissions-based estimate reported in AR5 by half a degree, owing to differences in forcing assumptions and ECS/TCR distributions."

Specific comments

Abstract

The comparison of the uncertainty bounds for ECS and TCE to those reported in AR5 is worth pointing out, but should be put in context since they are not based on the

same type of analysis. The AR5 range takes into account multiple lines of evidence, not just the type of study here, with a simple model constrained by observations.

Thank you for this comment. In retrospect the AR5 figures are a "likely" ($> 66\%$) range so we were in fact not comparing the same ranges. This sentence has been updated:

"The constrained estimates of equilibrium climate sensitivity (ECS), transient climate response (TCR) and transient climate response to cumulative CO_2 emissions (TCRE) are 2.93 (2.04 to 4.32) K, 1.59 (1.07 to 2.50) K and 1.44 (0.97 to 2.31) K (1000 GtC)$^{-1}$ (median and 5–95% credible intervals). These are in good agreement, with tighter uncertainty bounds, than the AR5 likely range, noting that AR5 estimates were derived from a combination of climate models, observations and expert judgement."

We have also updated the commentary in section 4.1 where these results are discussed.

The statement that the range of temperature projections under the RCP scenarios is lower in the FAIR model than those reported in AR5 is a significant outcome (especially depending on what the size of this difference actually is). The reasons for it (identified later in the paper) should also be included in the abstract.

As stated above, this has now been changed.

section 2

eq 3 is not explained as clearly as it could be. in what sense is IRF-100 associated with 100 years? The description seems to indicate that it is the cumulative atmospheric carbon load over 100 years following a pulse emission, and it is being equated to an expression depending on temperature and cumulative carbon uptake, but at an unspecified date in the future. The equation should make clearer the time variable, start/end times of a 100 year period, etc. It would also be useful to give the overall intuition of this approach. I assume it is that it relates the impulse response function time constants, which are derived in conditions that do not allow for representation of dependence on sink saturation and temperature feedback, to a situation in which those processes are acting. This allows derivation of the alpha parameter representing those effects.

You have the correct intuition for how this works. Equation 3 parametrises what would be the integrated additional carbon loading after 100 years ($iIRF_{100}$) in response to a one-time (strictly infinitesimal) pulse emission of CO_2 at the current point in time in the model's integration. Knowing $iIRF_{100}$ allows the scaling factor, α, on the model carbon cycle response timescales to be calculated. We parametrise the continuous evolution of $iIRF_{100}$ in response to this purely hypothetical pulse experiment to evolve with the present climate state. Numerically, this is implemented in equation 3, by using T and the cumulative carbon uptake from

the previous model timestep.

For methane and N2O, it seems like the approach is to specify a lifetime, and then adjust natural emissions over time so that historic concentrations are reproduced. Why is this preferable to specifying natural emissions, and estimating the lifetime that best fits the concentration data, leaving an unexplained error term that could represent variations in natural emissions or other errors (missing processes, error in anthropogenic emissions, etc.)? This is an example of where stating the general philosophy of the model might have helped, if the rationale is to use a lifetime provided in AR5. At a minimum some discussion of options and choices here is warranted.

Note that we have now updated the natural emissions to exactly balance the concentrations given anthropogenic emissions. It is our understanding that MAGICC does something akin to the reverse, where they start with concentrations and back out natural emissions given the anthropogenic emissions.

We have experimented with a constant natural emissions rate in model development. We find that the trajectory of historical concentrations is unrealistic (especially for methane), and this problem is confounded by using time-varying atmospheric lifetimes. Additionally, natural emissions are uncertain and vary interannually. The timeseries provided in figure 2 are the model defaults, and the user can specify their own.

You are correct that as far as possible we wanted to use AR5 estimates to inform the model. For methane this was not possible; using the 12.6 year lifetime in AR5 gives future emissions that are too high, whereas using 9.3 years gives the expected results both over the historical period (for a reasonable level of natural emissions) and in future, where they agree fairly well with the RCPs. We give some justification for this at the end of section 2.1.2.

Added: "We prefer to use varying natural emissions with a fixed atmospheric lifetime of CH_4 and N_2O, firstly because this provides a good match to observed and projected concentrations and secondly because this is consistent with the simple model philosophy. Other methods of calculating concentrations of these gases are possible, for example using a fixed natural background emission and relating any differences between observed and calculated historical concentrations as an error term (either in the natural or anthropogenic time series or missing processess), or by adjusting the atmospheric lifetime of each gas over the historical period in order to match the observed concentrations at each time step."

section 2.2.3: it is unclear how well the regression approach here captures the relationship observed in data or models. Some indication of the performance of this regression model should be given, along with best estimates of coefficients

As acknowledged in our response to the first reviewer, we have now moved from using a regression-based approach to one that is informed by estimates from ACCMIP models

(Stevenson et al., 2013). The evolution over the historical period is similar to AR5 up to around 1970 (fig. 5e in paper), after which the ACCMIP relationship results in a slightly stronger forcing than estimated by AR5 (but well within the uncertainty range in AR5).

The main difference is in the evolution of RCP8.5 past 2005 compared to the regression-based relationship which now shows a tropospheric forcing some 0.2 W m^{-2} higher than before. This is consistent with the modelling in Stevenson et al. (2013). The ozone forcing coefficients and year-2000 forcing values are provided in table 4.

2.2.4: it is noted that the functional relationship in eq 12 is from Meinshausen et al, however it is unclear if the rest of the approach (fitting to the AR5 ERF timeseries) is also the one taken by Meinshausen (or anyone else) in estimating parameters. Should be clarified what the source of the approach to the modeling and/or parameter estimation is, or whether it is new.

The function takes the same form as Meinshausen et al. (2011), as this was the best simple model that could be found in the literature. We do not know what the basis of their relationship is. By training our curve fit to the ERF AR5 time series we get a different parameter combination to Meinshausen et al. (2011).

We have updated this description:

"$a = -1.46 \times 10^{-5}$, $b = 2.05 \times 10^{-3}$ and $c = 1.03$ in eq. (12) are fitting parameters that are found by a least-squares curve fit between eq. (12) and the stratospheric ozone ERF timeseries from AR5; due to this data fitting approach, our parameters differ from MAGICC."

eq 15: as for eq 3, give some quantitative measure of how well this regression model explains the historical data (or show the scatter plot with the estimated model relationship)

As with tropospheric ozone, the aerosol forcing relationship has been updated to use established model results from Aerocom (for ERFari) and a simulator of the Ghan et al. (2013) model for ERFaci. The relationship of how each species affects ERFari (in terms of forcing per Mt emissions) and the ERFari in year 2011 is given in table 4.

The underlying model that calculates ERFaci is too slow to run in FAIR for large ensembles so was emulated based on emissions of SOx and primary organic aerosol (BC+OC). The relationship to precursor emissions and how it compares to Ghan's model is shown in figure S1.

2.2.9: The incorporation of the biophysical effect of land use change on forcing through albedo change may be useful, but it leaves out another important effect through changes to evapotranspiration, thus giving an incomplete accounting of biophysical

effects. The authors cite one study, with one climate model, which drew conclusions based only on historical land use change, to justify including only the albedo effect. Other models will reach different conclusions about the relative effects of these two processes. Also, the effects are latitude-dependent, and the Andrews study they cite notes that the albedo effect historically has been dominated by high latitude Northern Hemisphere changes in winter (dependent on snow cover). Thus the approach of a single coefficient relating land use to albedo forcing is questionable, given that the model is intended to be applied to a wide variety of scenarios in the future with different latitudinal distributions of land use, and probably changing snow cover.

At a minimum all of these issues should be acknowledged and discussed and the proposed approach relative to others (see eg Andy Jones paper at `https://link.springer.com/article/10.1007/s10584-015-1411-5`**) should be justified. The quality of the approximation described by eq 17 needs to be quantified.**

We appreciate our treatment of land use forcing may not include several important processes that occur in the real world that would only be possible by using an external gridded activity dataset (i.e. from LUH). However, the aim of the FAIR model is to produce a plausible projection tool with as little complexity as possible. The simpler the inputs to the model, the easier it will be for others to use it. To include gridded land processes would require something more complex than a zero dimensional model like an EMIC.

The basis for using this one coefficient was the observation that scaling with cumulative CO_2 land use emissions agrees remarkably well with the shape of the future forcing scenarios for the RCPs (compare dotted and solid coloured curves in fig. 5k) in MAGICC, whereas the fits to the historical data are not too bad. If MAGICC did use a more complex relationship, then it can be approximated very well with this simple formula. Although MAGICC may also contain errors and biases, we can show that the treatment of land use forcing in FAIR is no worse than in that model. We have expanded the discussion to include the points that you raise above.

The RMSE between the AR5 land use forcing and eq 17 is 0.012 W m^{-2} over the historical period.

2.3 Temperature change: The intro to this section notes that the approach differs slightly from FAIR 1.0, but earlier in the paper FAIR 1.0 is described as a carbon cycle model. If it also includes a simple climate model, that needs to be corrected in the text

FAIR v1.0 has a temperature change component included. The 4th paragraph in section 1 is updated (now “FAIR v1.0 is well-calibrated to the carbon cycle and temperatue response of earth system models”).

section 3: In this section some of the distributions from which parameter values are drawn are specified completely, others don't seem to be. All distrbituions should be fully specified, possibly in a table, and referred to from the text.

The ERF uncertainty ranges are given in table 1. Carbon cycle parameters are described in the text and are described as Gaussian, quoted as a mean and 90% uncertainty range. The section on ECS and TCR we have also re-written slightly and trust that it is now clearer.

For non-Gaussian ERF uncertainties the source of the original distributions are made more clear, e.g. AR5.

figure 4a: it would be useful if a separate plot with different scale could be shown for the historical period. With the y axis scale set to capture the full range in 2100, it is difficult to see any detail about the relation between the FAIR range and the observations.

An inset plot is now added to figure 4a which shows the historical period for CO_2 in more detail.

section 4.5: a more explicit description of the substantial differences in temperature change in 2100 between FAIR and Rogelj et al should be included. The differences in median temperature change are up to a full degree. Also, the high end of the range is very substantially truncated in FAIR, which would be extremely important to risk assessments. The text notes that they are different but underplays the size of the difference.

The new relationships we use for tropospheric ozone and aerosol forcing result in smaller temperature differences between FAIR and Rogelj et al. (2012), particularly in the lower RCPs. For RCP8.5, FAIR is around 0.5 K lower than Rogelj et al. (2012). This is still significant and a sentence has been added: "The difference of 0.5 K in the median end-of-century warming in RCP8.5 could be particularly important in policy assessments."

We have taken this opportunity to improve the readability of section 4.5. Some superfluous or no-longer-relevant sentences have been removed.

Table 5: section numbers referred to should all be in section 5, not 4.

Thank you for picking up on this reference to the old section numbering. It has now been updated.

Conclusions: it seems to me that the estimates of ECS and TCR (and future warming) are substantially more sensitive to the assumed priors than to other aspects of the analysis that are tested. The text here puts them all in the same category of showing "mild sensitivity". The alternative priors lead to a range of ECS/TCR that would reduce

the difference in the 95% level of projected 2100 warming by half, relative to Rogelj et al. No other sensitivity would have that large of an effect.

We agree: thank you for your suggestion. We have changed the description to highlight that the ECS, TCR and TCRE posteriors are fairly insensitive to the constraining dataset whereas they are more sensitive to the prior distribution.

In addition, here again the difference in projected warming by 2100 are very different from those in Rogelj et al, which seems worth emphasizing here. A full degree of warming difference in RCP8.5 is a substantial change in outlook.

For the updated model, these differences are smaller (0.5K in RCP8.5), so we do not change the main description as it stands but add a few words that provides this comparison.

References

Ghan, S. J., Smith, S. J., Wang, M., Zhang, K., Pringle, K., Carslaw, K., Pierce, J., Bauer, S., and Adams, P. (2013). A simple model of global aerosol indirect effects. *J. Geophys. Res.-Atmos.*, 118(12):6688–6707.

Meinshausen, M., Smith, S., Calvin, K., Daniel, J., Kainuma, M., Lamarque, J.-F., Matsumoto, K., Montzka, S., Raper, S., Riahi, K., Thomson, A., Velders, G., and van Vuuren, D. (2011). The RCP Greenhouse Gas Concentrations and their Extension from 1765 to 2300. *Climatic Change*.

Rogelj, J., Meinshausen, M., and Knutti, R. (2012). Global warming under old and new scenarios using IPCC climate sensitivity range estimates. *Nat. Clim. Change*, 2:248–253.

Stevenson, D. S., Young, P. J., Naik, V., Lamarque, J.-F., Shindell, D. T., Voulgarakis, A., Skeie, R. B., Dalsoren, S. B., Myhre, G., Berntsen, T. K., Folberth, G. A., Rumbold, S. T., Collins, W. J., MacKenzie, I. A., Doherty, R. M., Zeng, G., van Noije, T. P. C., Strunk, A., Bergmann, D., Cameron-Smith, P., Plummer, D. A., Strode, S. A., Horowitz, L., Lee, Y. H., Szopa, S., Sudo, K., Nagashima, T., Josse, B., Cionni, I., Righi, M., Eyring, V., Conley, A., Bowman, K. W., Wild, O., and Archibald, A. (2013). Tropospheric ozone changes, radiative forcing and attribution to emissions in the Atmospheric Chemistry and Climate Model Intercomparison Project (ACCMIP). *Atmos. Chem. Phys.*, 13(6):3063–3085.

FAIR v1.21: A simple emissions-based impulse response and carbon cycle model

Christopher J. Smith[1], Piers M. Forster[1], Myles Allen[2], Nicholas Leach[2], Richard J. Millar[3,4], Giovanni A. Passerello[1], and Leighton A. Regayre[1]

[1]School of Earth and Environment, University of Leeds, Leeds, UK
[2]Atmospheric Physics Department, University of Oxford, Oxford, UK
[3]College of Engineering, Mathematics and Physical Sciences, University of Exeter, Exeter, UK
[4]Environmental Change Institute, University of Oxford, Oxford, UK

Correspondence to: C.J.Smith (C.J.Smith1@leeds.ac.uk)

Abstract. Simple climate models can be valuable if they are able to replicate aspects of complex fully coupled earth system models. Larger ensembles can be produced, enabling a probabilistic view of future climate change. A simple emissions-based climate model, FAIR, is presented which calculates atmospheric concentrations of greenhouse gases and effective radiative forcing (ERF) from greenhouse gases, aerosols, ozone ~~precursors~~ and other agents. ~~The ERFs are integrated into global mean surface temperature change.~~ Model runs are constrained to observed temperature change from 1880 to 2016 and produce a range of future projections under the Representative Concentration Pathway (RCP) scenarios. ~~For the historical period the ERF time series in FAIR emulates the results in the IPCC Fifth Assessment Report (AR5), whereas for RCP historical and future scenarios, the greenhouse gas concentrations in FAIR closely track the observations and projections in the RCPs.~~ The constrained estimates of equilibrium climate sensitivity (ECS) ~~of 2.79 (1.97 to 4.08) K~~, transient climate response (TCR) ~~of 1.47 (1.03 to 2.23) K~~ and transient climate response to cumulative CO_2 emissions (TCRE) ~~of 1.43 (1.01 to 2.16) K (1000 GtC)$^{-1}$ (median and 5–95% credible intervals)~~ are 2.93 (2.04 to 4.32) K, 1.59 (1.07 to 2.50) K and 1.44 (0.97 to 2.31) K (1000 GtC)$^{-1}$ (median and 5–95% credible intervals). These are in good agreement, with tighter uncertainty bounds, than the AR5 likely range ~~(1.5 to 4.5 K, 1.0 to 2.5 K, and 0.8 to 2.5 K respectively),~~ noting that AR5 estimates were derived from a combination of climate models, observations and expert judgement. The ranges of future projections of temperature and ranges of estimates of ECS, TCR and TCRE are somewhat~~moderately~~ sensitive to the ~~historical temperature dataset used to constrain,~~ prior distributions of ECS/TCR parameters, but less sensitive to the~~aerosol radiative forcing relationship and~~ ERF from a doubling of CO_2 or the observational temperature dataset used to constrain the ensemble. Taking these sensitivities into account, there is no evidence to suggest that the median and credible range of observationally constrained TCR or ECS differ from climate model-derived estimates. The~~However, the~~ range of temperature projections under RCP8.5 ~~under the RCP scenarios~~ for 2081–2100 in the constrained FAIR model ensemble is~~are~~ lower than the emissions-based estimate~~s~~ reported in AR5 by half a degree, owing to differences in forcing assumptions and ECS/TCR distributions.

1 Introduction

Most multi-model studies, such as the Coupled Model Intercomparison Project (CMIP) which produces headline climate projections for the Intergovernmental Panel on Climate Change (IPCC) assessment reports, compare atmosphere-ocean general circulation models that are run with prescribed concentrations of greenhouse gases. Greenhouse gas and aerosol emissions time series are provided by integrated assessment modelling groups based on socio-economic narratives (Moss et al., 2010; Meinshausen et al., 2011b), which are then converted to atmospheric concentrations by simple climate-carbon-cycle models such as MAGICC6 (Meinshausen et al., 2011a). ~~EOn the other hand, e~~earth system models can be run in emissions mode, where emissions of carbon dioxide are used as a starting point and the atmospheric CO_2 concentrations are calculated interactively in the model~~. The earth system components of land and ocean carbon fluxes are based on biogeochemical relationships~~, with atmospheric concentration changes being the residual of emissions minus absorption by land and ocean sinks. While many models include the functionality to be run in CO_2 emissions-driven mode, these integrations were not the main focus of CMIP5 (the fifth phase of CMIP; Taylor et al. (2012)).

Earth system models in CMIP5 all show a positive carbon-cycle feedback, meaning that as surface temperature increases, land and ocean carbon sinks become less effective at absorbing CO_2 and a larger proportion of any further emitted carbon will remain in the atmosphere (Friedlingstein, 2015). The various feedback strengths are nevertheless ~~very~~ model dependent (Friedlingstein et al., 2006)~~. The causes of model diversity in feedback strengths was explored only superficially in CMIP5 owing to the number of earth system models available and the experimental design (Taylor et al., 2012; Millar et al., 2017). Only CO_2-emission driven experiments under historical and RCP8.5 forcing compared to pre-industrial control emissions were core experiments in CMIP5 for emissions-driven earth system models (Taylor et al., 2012).~~ While CO_2 is the most important climate forcer, individual models may also differ in their responses to non-CO_2 forcings~~respond differently to other emissions~~. These forcings can also introduce uncertainty that is not captured in concentration-driven or CO_2-only driven model experiments (Matthews and Zickfeld, 2012; Tachiiri et al., 2015). As non-CO_2 forcing impacts temperature which affects the efficiency of carbon sinks, non-CO_2 forcing agents themselves influence the carbon cycle (MacDougall et al., 2015).

Simple models can be used to emulate radiative forcing and temperature responses to emissions and atmospheric concentrations, and can be tuned to replicate the behaviour of individual climate and earth system models (Meinshausen et al., 2011a; Good et al., 2011, 2013; Geoffroy et al., 2013). In the IPCC Fifth Assessment Report (AR5), a simple carbon-cycle model was suggested, calibrated to present-day conditions (Supplementary Material to Myhre et al., 2013b). This model used fixed time constants for the decay of atmospheric CO_2 where time constants were taken from a multi-model intercomparison of full- and intermediate-complexity earth system ~~and~~ models (Joos et al., 2013) with no feedbacks assumed for biospheric carbon uptake or temperature. It was introduced for the purposes of calculating global warming potentials, built on the impulse response model of Boucher and Reddy (2008). Millar et al. (2017) showed that this AR5 model does not sufficiently capture the time-evolving dependency of carbon sinks with cumulative carbon emissions and temperatures. They introduced the Finite Amplitude Impulse Response (FAIR) model (version 1.0) that tracks the time-integrated airborne fraction of carbon and uses

this to determine the efficiency of carbon sinks, in turn calculating atmospheric CO_2 concentrations, radiative forcing, and temperature change. ~~This model, version 1.1, is developed further in this paper.~~

~~Simple models themselves span a range of complexity scales. At one end are one-box and multi-box impulse response models , and at the other are models that treat land and ocean processes separately, with sophisticated carbon cycles, state-varying atmospheric sinks and ocean upwelling-diffusion modelling . Providing that simple models can adequately capture the key features of more complex climate and earth system models, they can be used to create ensemble estimates of future scenarios that would not be possible due to computational demands, and provide the capacity for probabilistic interpretations of future climate change.~~

FAIR v1.0 ~~a simple CO_2 emissions-based carbon cycle model, written in Python 2, that~~ is well-calibrated~~validated~~ to the temperature and carbon cycle response of earth system models. FAIR v1.2~~1~~ is extended to calculate non-CO_2 greenhouse gas concentrations from emissions, aerosol forcing from aerosol precursor emissions, tropospheric and stratospheric ozone forcing from the emissions of precursors, and forcings from black carbon on snow, stratospheric methane oxidation to water vapour, contrails and land use change. ~~Although many of these forcings exhibit substantial regional variations, this is expected to be smoothed out in the global mean.~~ Forcings from volcanic eruptions and solar irradiance fluctuations are supplied externally. These forcings are then converted to a temperature change, taking into account the different thermal responses of the ocean mixed layer and deep ocean.

The model philosophy in FAIR is to represent these processes as simply as possible, and to be able to emulate the historical ERF time series in AR5 given input emissions. FAIR is written in Python and open source. The extension to non-CO_2 emissions makes FAIR v1.2~~1~~ applicable for assessing scenarios with a broad range of emissions pathways~~commitments~~.

This paper introduces the FAIR model in section 2, including the key changes from versions 1.0 to 1.2~~1~~.1. Section 3 then discusses the generation of a large ensemble of input parameters to the FAIR model which is run and results described in section 4. A sensitivity analysis to some of the key inputs to the large ensemble is given in section 5. Section 6 provides a summary.

2 Development of FAIR v1.2~~1~~ and differences to v1.0

FAIR v1.2~~1~~ takes emissions of greenhouse gases and~~,~~ short-lived climate forcers as its main input. This is an array of size (number of years $\times$ 40) (see table 1), and is based on the order provided in the RCP emissions datasets (Meinshausen et al., 2011b). Additional inputs that can be specified by the user are~~,~~ the fraction of total nitrogen oxides (NOx) emitted by the aviation sector, fraction of total methane attributable to fossil fuels, natural emissions of CH_4 and N_2O, and natural forcing from solar variability and volcanoes~~, as its inputs~~. The atmospheric concentrations of greenhouse gases are calculated from new emissions minus the decay of the current atmospheric burden, which is determined by the atmospheric lifetime of each gas, and output as a (years $\times$ 31) array (table 2). For CO_2, atmospheric concentrations are calculated from a simple representation of the carbon cycle which includes temperature and saturation dependency of land and ocean sinks and includes a proportion of methane oxidised to CO_2. The effective radiative forcing (ERF) from 13 different forcing agents (table 3) is determined

from the concentrations of each greenhouse gas, plus emissions of short-lived climate forcers and natural forcing and is output from the model as a (years × 13) array. From the ERF, temperature change is calculated. The change in temperature feeds back into the carbon cycle, which impacts the atmospheric lifetime of carbon dioxide. A flow diagram outlining the key processes is provided in fig. 1. It is also possible to run FAIR using only CO_2 emissions as inputs, where a time series of non-CO_2 forcing can be optionally specified rather than calculated from emissions.

2.1 Greenhouse gases: emissions to concentrations

2.1.1 Carbon dioxide and carbon cycle

The carbon cycle component in FAIR v1.0 is described in detail by Millar et al. (2017) and an overview is provided here. The FAIR model uses anthropogenic fossil and land-use CO_2 emissions as input and partitions them into four boxes R_i (with partition fraction a_i and $\sum_0^3 a_i = 1$) representing the differing time scales of carbon uptake by geological processes (τ_0), the deep ocean (τ_1), biosphere (τ_2) and ocean mixed layer (τ_3). The atmospheric concentrations of CO_2 and its relationship to each box is

$$C_{\mathrm{CO_2}} = C_{\mathrm{CO_2,pi}} + \sum_{i=0}^{3} \frac{R_i}{M_a} \frac{w_{\mathrm{CO_2}}}{w_a} \tag{1}$$

with $C_{\mathrm{CO_2,pi}}$ equal to 278 ppm and pi representing pre-industrial. $M_a = 5.1352 \times 10^{18}$ kg is the dry mass of the atmosphere and $w_{\mathrm{CO_2}}$ and w_a are the molecular weights of CO_2 and dry air. R_i is in kilograms. The governing equations for the four boxes are

$$\frac{\mathrm{d}R_i}{\mathrm{d}t} = a_i E_{\mathrm{CO_2}} - \frac{R_i}{\alpha \tau_i}; \qquad i = 0, \ldots, 3 \tag{2}$$

with $E_{\mathrm{CO_2}}$ the emissions of CO_2.

The four time constants τ_i are scaled by a factor α depending on the 100-year integrated impulse response function ($\mathrm{iIRF_{100}}$), which represents the 100-year average airborne fraction of a pulse of CO_2 (Joos et al., 2013). α is found by equating two different expressions for $\mathrm{iIRF_{100}}$

$$\sum_{i=0}^{3} \alpha a_i \tau_i \left[1 - \exp\left(\frac{-100}{\alpha \tau_i}\right)\right] = r_0 + r_C C_{\mathrm{acc}} + r_T T \tag{3}$$

and finding the unique root α (Millar et al., 2017). The right hand side of eq. (3) proposed by Millar et al. (2017) is a simplified expression for $\mathrm{iIRF_{100}}$ that depends on the total accumulated carbon in land and ocean sinks $C_{\mathrm{acc}} = (\sum_t E_{\mathrm{CO_2},t}) - (C_{\mathrm{CO_2}} - C_{\mathrm{CO_2,pi}})$ and temperature change T since the pre-industrial era that simulates the behaviour of earth system models well. This increase in $\mathrm{iIRF_{100}}$ and scaling of the time constants by α accounts for the land and ocean carbon sinks changing absorption efficacy~~approaching saturation~~ as more carbon is added to them (r_C parameter). In earth system models it is also observed that the efficiency of carbon sinks decreases with increasing temperature (r_T parameter; Fung et al. (2005); Friedlingstein et al. (2006)). Following Millar et al. (2017) we use $r_C = 0.019$ yr GtC^{-1} and $r_T = 4.165$ yr K^{-1}, but in contrast to Millar et al.

(2017) a pre-industrial $r_0 = 35$ years is used rather than their 32.4 years. This facilitates better agreement with present-day CO_2 atmospheric concentrations when spun up from 1765 with historical CO_2 and non-CO_2 emissions. This parameter combination is consistent with a present-day $iIRF_{100}$ diagnosed from more complex carbon-cycle models (Joos et al., 2013) with a fixed backgroundreference CO_2 concentration of 389 ppm.

2.1.2 Other greenhouse gases

A one-box decay model is assumed for other greenhouse gases where the sink is an exponential decay of the existing gas concentration anomaly. New emissions are converted to concentrations in year t by

$$\delta C_t = \frac{E_t}{M_a}\frac{w_a}{w_f}\delta_t \tag{4}$$

where E_t is the emissions of gas in year t, $M_a = 5.1352 \times 10^{18}$ kg is the mass of the atmosphere and w_f is the molecular mass of the greenhouse gas ($\delta_t = 1$ for annual emissions data). The model updates the atmospheric concentrations at year t based on new emissions and the natural sink by

$$C_t = C_{t-1} + \frac{1}{2}(\delta C_{t-1} + \delta C_t) - C_{t-1}(1 - \exp(-1/\tau)) \tag{5}$$

where τ is the atmospheric lifetime of each gas (table 2).

For CH_4 and N_2O, time-varying natural emissions are included in E_t (fig. 2) in order to closely match the observed atmospheric concentrations of these gases in Meinshausen et al. (2011b), including the 1765 concentrations when the 1765 natural emissions are run to steady state. The time series of natural emissions used include abrupt step changes in places in order to counterbalance differing rates of change in anthropogenic emissions, for example a rapid increase in anthropogenic N_2O emissions in the 1940s. Beyond 2005, In 2011 the natural emissions of CH_4 and N_2O are fixed attaken as 191195 Mt CH_4 yr^{-1} and 8.998.75 Mt N_2-eq yr^{-1} which are close to the best-estimate present-day emissions of 202 Mt CH_4 yr^{-1} and 9.1 Mt N_2-eq yr^{-1} (Prather et al., 2012). We prefer to use varying natural emissions with a fixed atmospheric lifetime of CH_4 and N_2O, firstly because this provides a good match to observed and projected concentrations and secondly because this is consistent with the simple model philosophy. Other methods of calculating concentrations of these gases are possible, for example using a fixed natural background emission and relating any differences between observed and calculated historical concentrations as an error term (either in the natural or anthropogenic time series or missing processes), or by adjusting the atmospheric lifetime of each gas over the historical period in order to match the observed concentrations at each time step.

Natural emissions of CO_2 are not included as the carbon cycle model is more complex than the single box used for other gases and it is assumed that natural sources and natural sinks are in balance. For other greenhouse gases, natural emissions are assumed to be zero except for CF_4, CH_3Br and CH_3Cl. Pre-industrial concentrations of these three minor compounds are estimated by running the 1765 emissions from Meinshausen et al. (2011b) to steady state using the lifetimes in table 2. Unlike CH_4 and N_2O, natural emissions of CF_4, CH_3Br and CH_3Cl are included in the anthropogenic emissions data.Rather than using the pre-industrial emissions for these three species in Meinshausen et al (2011b), we instead match the pre-industrial concentrations in Meinshausen et al (2011b) by running eq. (5) to steady state with the atmospheric lifetimes from table 3. We

~~obtain background natural emissions of 0.0109 kt CF_4 yr^{-1}, 69.7 kt CH_3Br yr^{-1} and 2716 kt CH_3Cl yr^{-1}. The Meinshausen et al (2011b) emissions are then adjusted by adding on these background values of these three species and subtracting the Meinshausen et al (2011b) year-1765 emissions from all years.~~ In total, 31 greenhouse gas species are used (table 2). Other than CO_2, CH_4 and N_2O, the remaining gases can be subdivided into those covered by the Kyoto Protocol (HFCs, PFCs, SF_6), and the ozone depleting substances (ODSs) covered by the Montreal Protocol (CFCs, HCFCs and other chlorinated and brominated compounds).

The best estimate of τ for each gas except methane is used from AR5 (Myhre et al., 2013b, table 8.A.1), consistent with using AR5 estimates for parameters where possible. We find that using a constant methane lifetime of 9.3 years results in reasonable levels of historical natural emissions and also agrees well with the MAGICC6-projected RCP concentration scenarios in the future~~with small variations to the natural emissions provides a time series of historical atmospheric methane concentrations that differs from Meinshausen et al (2011b) by at most 1.2% and usually much less~~. The methane lifetime of 9.3 years used is significantly lower than the 12.4 years in AR5. This latter figure includes the feedback of methane emissions on its own lifetime (a factor of 1.34; Holmes et al. (2013), also used in AR5) and is used for perturbation calculations against a constant background concentration. Dividing the perturbation lifetime by 1.34 gives the atmospheric burden lifetime of 9.3 years.

2.1.3 Methane oxidation to CO_2

The oxidation of CH_4 produces additional CO_2 if it is of fossil origin, which is~~and this has also been~~ accounted for in the model. Methane is assumed to be from fossil sources if it ~~is of anthropogenic origin and~~ arises from the transport, energy or industry sectors. We use the breakdown of emissions by sector from the RCP Database (2009) . A best estimate of 61% of the methane lost through reaction with the hydroxyl radical in the troposphere (the dominant loss pathway) is converted to CO_2 (Boucher et al., 2009). This is treated as additional emissions of CO_2:

$$E_{CH_4 \rightarrow CO_2} = 0.61 f_{CH_4 fos} (C_{CH_4} - C_{CH_4,pi})(1 - \exp(-1/\tau_{CH_4})) \quad (6)$$

where $f_{CH_4 fos}$ is the fraction of anthropogenic methane attributable to fossil sources and τ_{CH_4} is 9.3 years. As atmospheric methane concentrations are reduced by exponential decay in eq. (5), this prevents against (approximately) double-counting an emitted fossil-fuel CH_4 molecule as both CH_4 and CO_2 after it has been oxidised.

Oxidation of CO and non-methane volatile organic compounds (NMVOCs) to CO_2 is not included as to not double count the carbon that is included in national CO_2 emissions inventories (Daniel and Solomon, 1998; Gillenwater, 2008).

2.2 Effective radiative forcing

The ERF from 13 different forcing agent groups are considered: CO_2, CH_4, N_2O, other greenhouse gases, tropospheric O_3, stratospheric O_3, stratospheric water vapour, contrails, aerosols, black carbon on snow, land use change, solar irradiance and volcanoes (table 3). ERF, which accounts for all (stratospheric plus tropospheric) rapid adjustments, corresponds better to temperature change than "traditional" stratospherically adjusted radiative forcing (RF) (Myhre et al., 2013b; Forster et al., 2016). Therefore, we use relationships for ERF where they exist.

2.2.1 Carbon dioxide, methane and nitrous oxide

We use the updated Etminan et al. (2016) RF relationships for CO_2, CH_4 and N_2O, which for the first time includes band overlaps between CO_2 and N_2O. It also includes a significant upward revision of the CH_4 RF due to inclusion of previously neglected shortwave absorption, compared to the previous relationships of Myhre et al. (1998) used in AR5. Although Etminan et al. (2016) calculate RF, Myhre et al. (2013b) concluded~~showed~~ that over the industrial era there was not sufficient evidence to state that ERF was significantly different from~~ERF agrees with~~ RF for these three gases, and ERF is taken to equal RF, although with a doubled uncertainty range. The Etminan et al. (2016) relationships are reproduced in eqs. (7) to (9), where C (ppm), M and N (ppb) have been used to represent concentrations of CO_2, CH_4 and N_2O, and the subscript pi representing pre-industrial concentrations.

$$F_{\mathrm{CO_2}} = \left[(-2.4\times10^{-7})(C-C_{\mathrm{pi}})^2 + (7.2\times10^{-4})|C-C_{\mathrm{pi}}| - (1.05\times10^{-4})(N+N_{\mathrm{pi}}) + 5.36\right] \times \log\left(\frac{C}{C_{\mathrm{pi}}}\right) \quad (7)$$

$$F_{\mathrm{N_2O}} = \left[(-4.0\times10^{-6})(C+C_{\mathrm{pi}}) + (2.1\times10^{-6})(N+N_{\mathrm{pi}}) - (2.45\times10^{-6})(M+M_{\mathrm{pi}}) + 0.117\right] \times \left(\sqrt{N} - \sqrt{N_{\mathrm{pi}}}\right) \quad (8)$$

$$F_{\mathrm{CH_4}} = \left[-(6.5\times10^{-7})(M+M_{\mathrm{pi}}) - (4.1\times10^{-6})(N+N_{\mathrm{pi}}) + 0.043\right] \times \left(\sqrt{M} - \sqrt{M_{\mathrm{pi}}}\right). \quad (9)$$

Finally, a scaling to $F_{\mathrm{CO_2}}$ is made to ensure that a doubling of CO_2 using eq. (7) along with pre-industrial N_2O concentrations equals the user-specified value of $F_{2\times}$, which defaults to 3.71 W m^{-2}.

2.2.2 Other well-mixed greenhouse gases

For all well-mixed greenhouse gases in table 2 except CO_2, CH_4 and N_2O the ERF is assumed to be a linear relationship of the change in gas concentration C_i since the pre-industrial era by its radiative efficiency η_i [W m^{-2} ppb]:

$$F_i = \eta_i(C_i - C_{i,\mathrm{pi}}); \qquad i \in \{\text{gas indices} \quad 3,4\ldots,30\} \quad (10)$$

where radiative efficiencies are given in table 2, i refers to index numbers in table 2 and C_i are converted to ppb. This is an established method for small greenhouse gas forcings, also used in MAGICC.

2.2.3 Tropospheric ozone

Tropospheric ozone is formed from a complex chemical reaction chain from emissions of CH_4, NOx, CO and NMVOC. Furthermore its concentration is more variable in space and time than for the well-mixed greenhouse gases. Therefore, we do not calculate a globally averaged concentration. We use coefficients from Stevenson et al. (2013) to estimate tropospheric ozone ERF from emissions of NOx, CO and NMVOC, and concentrations of methane, assuming linearity between atmospheric burden and ozone forcing:~~We use a multivariate linear regression between the emissions of CH_4, NOx, CO and NMVOC (predictors) and tropospheric ozone ERF diagnosed in AR5 such that~~

$$F_{\mathrm{O_3tr}} = \beta_{\mathrm{CH_4}}(C_{\mathrm{CH_4}} - C_{\mathrm{CH_4,pi}}) + \beta_{\mathrm{NOx}}(E_{\mathrm{NOx}} - E_{\mathrm{NOx,pi}}) + \beta_{\mathrm{CO}}(E_{\mathrm{CO}} - E_{\mathrm{CO,pi}}) + \beta_{\mathrm{NMVOC}}(E_{\mathrm{NMVOC}} - E_{\mathrm{NMVOC,pi}}) + f(T) \quad (11)$$

and

$$f(T) = \min\{0, 0.032\exp(-1.35T) - 0.032\} \tag{12}$$

The β coefficients in eq. (11) are provided in table 4 and eq. (12) is a small negative climate feedback, estimated using a curve fit to year 2000, 2030 and 2100 temperature changes under RCP8.5 in Stevenson et al. (2013). As Stevenson et al. (2013) used 1850 as their baseline for forcing calculations based on emissions data from Lamarque et al. (2010), in RCP scenarios adjusted coefficients can optionally be specified for times prior to 1850 where "pre-industrial" anthropogenic emissions are taken from Skeie et al. (2011). This ensures that ERF is both equal to zero in 1765 and equal to the best estimates in Stevenson et al. (2013) for 2005. Both the differing treatment prior to 1850 and the climate feedback can optionally be switched off by the user.

~~Only anthropogenic CH_4 emissions are considered in eq. (11), defining tropospheric ozone changes in FAIR as a purely anthropogenic forcing. The regression approach has the effect of isolating the effect of each precursor species on its total contribution to the tropospheric ozone forcing. The regression coefficients $\beta_{CH_4} = 2.82 \times 10^{-4}$, $\beta_{NOx} = 99.78 \times 10^{-4}$, $\beta_{CO} = 1.07 \times 10^{-4}$ and $\beta_{NMVOC} = -9.36 \times 10^{-4}$ W m^{-2} (Mt yr^{-1})$^{-1}$. Unlike Stevenson et al. (2013) we find a negative correspondence on ozone forcing with emissions of NMVOC with this simplified method. All other emissions species result in a positive tropospheric ozone forcing.~~

2.2.4 Stratospheric ozone

The stratospheric ozone ERF is calculated using the functional relationship borrowed from~~in~~ Meinshausen et al. (2011a), namely

$$F_{O_3 st} = a(bs)^c. \tag{13}$$

$a = -1.46 \times 10^{-5}$, $b = 2.05 \times 10^{-3}$ and $c = 1.03$ in eq. (13) are fitting parameters that are found by a least-squares curve fit between eq. (13) and the stratospheric ozone ERF timeseries from AR5; due to this data fitting approach, our parameters differ from MAGICC. s is the equivalent effective stratospheric chlorine (EESC) from all ozone depleting substances, calculated as (Newman et al., 2007)

$$s = r_{CFC11} \sum_{i \in ODS} \left(n_{Cl}(i) C_i \frac{r_i}{r_{CFC11}} + 45 n_{Br}(i) C_i \frac{r_i}{r_{CFC11}} \right). \tag{14}$$

r_i represents fractional release values for each ODS compound taken from Daniel and Velders (2011) and reproduced in table 2. n_{Cl} and n_{Br} represent the number of chlorine and bromine atoms in compound i with the factor of 45 in eq. (14) indicating that bromine is 45 times more effective at stratospheric ozone depletion than chlorine (Daniel et al., 1999). The concentrations C_i are expressed in ppb ~~and are taken from year $t-3$, representing the time for the air to be transported to the stratosphere~~.

2.2.5 Stratospheric water vapour from methane oxidation

In AR5, the ERF from the stratospheric water vapour oxidation of methane was assumed to be 15% of the methane ERF. This was based on the methane forcing relationship of Myhre et al. (1998), which is about 20% lower than the Etminan et al. (2016)

methane forcing used in FAIR. As there has been no substantial revision to the stratospheric water vapour forcing we define stratospheric water vapour ERF as 12% of the methane ERF ~~This approach is also taken in FAIR~~.

2.2.6 Contrails

Meinshausen et al. (2011b) did not include a forcing timeseries for contrails or contrail-induced cirrus, which contribute a small positive ERF (Boucher et al., 2013). It is assumed that contrail ERF is proportional to the level of air traffic, which is in turn is proportional to aircraft emissions (Lee et al., 2009). We use aviation NOx emissions for this purpose, which are obtained from the RCP database. The ERF from contrails F_{con} is scaled by the ratio of aircraft NOx emissions in a given year compared to 2011 and multiplied by the 2011 ERF:

$$F_{\text{con}} = \frac{E_{\text{NOx,avi}}}{E_{\text{NOx,avi,2011}}} F_{\text{con,2011}}. \tag{15}$$

This gives a coefficient of $F_{\text{con,2011}}/E_{\text{NOx,avi,2011}} = 0.0152$ W m^{-2} (Mt-aviNOx yr^{-1})$^{-1}$.

2.2.7 Aerosols

~~The radiatively active aerosols in the RCP datasets are fossil fuel black carbon (BC), fossil fuel organic carbon (OC), sulfate, nitrate, biomass aerosol and mineral dust.~~ Aerosols have a lifetime of the order of days (Kristiansen et al., 2016), and the emissions are converted to forcing without an intermediate concentration step.

The aerosol ERF contains contributions from aerosol-radiation interactions (ERFari) and from aerosol-cloud interactions (ERFaci). ERFari includes the direct radiative effect of aerosols, in addition to rapid adjustments due to changes in the atmospheric temperature, humidity and cloud profile (formerly the semi-direct effect; Boucher et al. (2013)).

We use the multi-model results from Aerocom (Myhre et al., 2013a) to provide coefficients of how emissions affect ERFari. Again we assume a linear relationship between emissions and forcing:

$$F_{\text{ari}} = \gamma_{\text{BC}} E_{\text{BC}} + \gamma_{\text{OC}} E_{\text{OC}} + \gamma_{\text{SOx}} E_{\text{SOx}} + \gamma_{\text{NOx}} E_{\text{NOx}} + \gamma_{\text{NH}_3} E_{\text{NH}_3} + \gamma_{\text{SOA}} E_{\text{NMVOC}} \tag{16}$$

where the coefficients for each γ are provided in table 5 and calculated from the difference in anthropogenic emissions between 1850 and 2000 (Lamarque et al., 2010) and scaled for rapid adjustments (see below). We assume emitted black carbon (BC) and organic carbon (OC) correspond directly to BC and OC forcing, and that emissions of sulfur compounds (SOx) correspond directly to sulfate forcing. Following Shindell et al. (2009) we assume a 60% contribution to nitrate aerosol forcing from NH_3 and 40% from NOx. We allow formation of secondary organic aerosol (SOA) to scale with emissions of anthropogenic NMVOC. Biomass burning aerosol has a net zero forcing in 2011 and is ignored, and mineral dust, which does not scale directly with an emitted component, is also disregarded. The sum of the direct effects of each component is -0.328 W m^{-2} in 2011 assuming RCP4.5. The difference between this and the best estimate ERFari of -0.45 W m^{-2} in AR5 is assumed to be due to rapid adjustments (semi-direct effects), and therefore the radiative efficiency of each species is scaled by a factor of 1.37.

~~In the AR5 ERF time series, the components of aerosol forcing are not considered separately, but the year 2011 best estimates of -0.45 W m^{-2} for ERFari and -0.45 W m^{-2} ERFaci are given.~~

~~We use a multi-linear regression approach to isolate the effect of each emitted species (BC, OC, SOx, NOx and NH_3) on the total aerosol forcing by regressing the AR5 historical time series against the emissions in Meinshausen et al. (2011b):~~

~~To provide bounds on the contribution of each species to the total aerosol forcing, we use the maximum and minimum of the multi-model radiative forcing results from Aerocom (Myhre et al., 2013a) for the direct forcing of each species. The sum of direct forcing is -0.31 W m^{-2} for the best estimate from Aerocom models, so the upper bounds (i.e. furthest bound from zero) of each species is scaled by $-0.9/-0.31$ to account for the rapid adjustments in ERFari and ERFaci that contribute to the total aerosol forcing. This leads to the estimates of 2011 ERF and regression coefficients in table 4.~~

~~In this simplified treatment the ERF in 2011 for BC and sulfate are towards the weaker end of the allowable range (the range guided by Aerocom models, scaled for adjustments) while the ERFs from nitrate aerosol precursors are at the most extreme strong end. We also assume that the relationship between aerosol ERF and emissions is linear, and do not discriminate on the strength of adjustments by species. There is some evidence to suggest that the aerosol forcing may increase as a sub-linear, potentially logarithmic, function of emissions as the increase in cloud albedo, one component of ERFaci, saturates with increasing aerosol emissions (Twomey, 1991; Carslaw et al., 2013). An alternative relationship is explored in the sensitivity analysis.~~

ERFaci describes how aerosols affect clouds in the radiation budget; the two main mechanisms are changes in cloud droplet size, which changes cloud albedo (Twomey, 1977) and changes in cloud lifetime and precipitation efficiency which affects cloud fraction (Albrecht, 1989; Boucher et al., 2013). There is evidence that the ERFaci is not linear with emissions (Carslaw et al., 2013) and as such a simple linear scaling as for ERFari may not be appropriate.

In FAIR we use an emulation of the global aerosol model of Ghan et al. (2013) to estimate ERFaci from precursor emissions. The Ghan et al. (2013) method contains a series of non-linear equations that require iterative solutions and currently has not been optimised for use in FAIR. We therefore emulate the ERFaci by varying the emissions of SOx and primary organic aerosol (the sum of BC and OC). Secondary organic aerosol is also an input to the model, but it is found that ERFaci is only weakly dependent on NMVOC emissions and a simple functional form could not be found, so was eliminated as a predictor.

Informed by the simple aerosol model of Stevens (2015), we use a logarithmic dependence of ERFaci on emissions that can vary both as a function of SOx and BC+OC, which represents increasing saturation of the cloud-albedo effect with increasing emissions. We find a relationship of the form

$$G(E_{\mathrm{SOx}}, E_{\mathrm{BC+OC}}) = -1.95 \log(1 + 0.0111 E_{\mathrm{SOx}} + 0.0139 E_{\mathrm{BC+OC}}) \tag{17}$$

where the coefficients in eq. (17) are found with a least-squares optimisation routine ($r^2 = 0.938$). The modelled and simulated outputs are compared in figure S1.

Equation (17) was derived from a climate model, and produces a present-day ERFaci that is stronger than the central estimate of -0.45 W m^{-2} from AR5. We therefore scale eq. (17) in order to obtain a forcing of -0.45 W m^{-2} in 2011 under RCP4.5

emissions:

$$F_{\text{aci}} = -0.45\frac{G(E) - G(E_{1765})}{G(E_{2011}) - G(E_{1765})} \tag{18}$$

where $E = (E_{\text{SOx}}, E_{\text{BC+OC}})$ refers to emissions, and a numerical subscript refers to a particular year. The emissions for 1750 from Skeie et al. (2011) are used for year 1765, and a linear interpolation between 1765 and 1850 applied.

2.2.8 Black carbon on snow

The best -estimate ERF of 0.04 W m^{-2} in AR5 for 2011 is compared to the BC emissions in 2011 from Meinshausen et al. (2011b), with this scaling factor assumed to hold for all years. The relationship is given by

$$F_{\text{BCsnow}} = 0.00494E_{\text{BC}}, \tag{19}$$

where E_{BC} is BC emissions in Mt yr^{-1}.

2.2.9 Land use change

Land use forcing is a result of ~~is largely driven by~~ surface albedo change (Andrews et al., 2017) and changes in evapotranspiration patterns (Jones et al., 2015), which is often due to deforestation for agriculture (Myhre and Myhre, 2003). Cropland has a higher albedo than the forest that it replaces, reflecting more incident solar radiation and therefore resulting in a negative ERF; additionally, deforestation in boreal regions may unmask snow-covered ground, again increasing albedo.

Deforestation produces land-use related CO_2 emissions. The total amount of deforestation since pre-industrial times could therefore be expected to scale with cumulative land-use related CO_2 emissions. This approach is taken in FAIR. A regression of non-fossil CO_2 emissions against land use ERF in AR5 gives

$$F_{\text{landuse}} = -1.14 \times 10^{-3} \sum_{j=0}^{t} E_{\text{CO}_2\text{land},j}, \tag{20}$$

where the coefficient has units W m^{-2} (Gt C)$^{-1}$.

The simple relationship in eq. (20) does not take into account latitude dependence of surface albedo or any evapotranspiration changes. As a zero-dimensional model, FAIR does not include geographical dependence of individual forcing effects, which may differ significantly between forcing pathways (for example the scenarios typically used to drive integrated assessment models). Inclusion of evapotranspiration effects, again which differ between tropical and boreal regions (Jones et al., 2015), is challenging as they do not directly relate to an emitted species or a change in radiative forcing (Pielke et al., 2002). Nevertheless, we conclude that this simple treatment is acceptable, firstly as the range of land use forcing uncertainty is relatively large (so much that the sign of the forcing is not known with confidence (Myhre et al., 2013b)), secondly because at least in the best estimate the forcing is a small fraction of the present-day total, and thirdly because the future trajectory of the land use forcing in the RCP datasets is very similar to that predicted by FAIR, suggesting that a dependence on cumulative land-use CO_2 emissions is an important component of the land use forcing in MAGICC.

2.2.10 Solar variability

The SOLARIS-HEPPA v3.2 solar irradiance dataset prepared for CMIP6 is used to generate the solar ERF, which includes projections of the variation in future solar cycles from 1850 to 2300 (Matthes et al., 2017). ERF from solar forcing is calculated as the change in solar constant since 1850 divided by 4 (average insolation) and multiplied by 0.7 (representing planetary co-albedo). This approach is also used in Meinshausen et al. (2011b). Prior to 1850, we revert to the solar forcing from AR5.

2.2.11 Volcanic aerosol

Historical volcanic forcing is punctuated by several large eruptions that cause large but short-lived negative forcing episodes, with several smaller eruptions that cause year-to-year changes in the volcanic forcing. In order to generate a historical volcanic ERF time series we first start with gridded volcanic optical depths taken from the Easy Volcanic Aerosol generator over the 1850–2014 period (Toohey et al., 2016) which will be used to drive CMIP6 models. A number of time slice experiments with various scalings of the historical mean volcanic optical depth are run in the HadGEM3-GA7.1 climate model (Walters et al., 2017), where it was found that aerosol ERF scales as $-18\tau_{\text{vol}}$ (where τ_{vol} is globally averaged volcanic aerosol optical depth at 550 nm). This scaling factor is consistent with other HadGEM models (Gregory et al., 2016), although weaker than the value of $-26\tau_{\text{vol}}$ adopted in AR5. The discrepancy is claimed to be due to rapid adjustments, in which case our adoption of the less negative value is consistent with the ERF definition.

In the context of measuring forcing since the pre-industrial, we have to assume an "average" level of volcanic background aerosol. We therefore define the 1850–2014 period to have a mean volcanic forcing of zero. To achieve this we subtract the mean (negative) forcing from the historical period, resulting in a quiescent year ERF of around $+0.1$ W m^{-2}. A similar approach was taken in Meinshausen et al. (2011b), with a higher quiescent year forcing of about $+0.2$ W m^{-2}. Prior to 1850 we use the AR5 dataset, scaled by 18/26 to match the differences in optical depth/forcing relationships, and from 2015 onwards volcanic forcing is defined to be zero.~~The ERF from volcanic eruptions in AR5 is used without modification.~~ For solar and volcanic forcing, users are free to provide a custom forcing time series or to use the AR5 or RCP datasets which are both available in FAIR.

2.3 Temperature change

In simple impulse-response models, forcing is related to total temperature change in year t, T_t, by a two-time constant model (Boucher and Reddy, 2008; Myhre et al., 2013b; Millar et al., 2015, 2017). FAIR v1.2~~1~~ takes this approach with a small modification compared to FAIR v1.0 to allow for forcing-specific efficacies ϵ_j such that

$$T_{t,i} = T_{t-1,i}\exp(1/d_i) + \sum_{j=0}^{12}(q_i\epsilon_j F_j(1-\exp(1/d_i)); \qquad i = 1,2. \tag{21}$$

Owing to the use of ERF rather than RF in FAIR v1.2~~1~~ and its better correspondence with temperature, efficacies are assumed to be unity for all forcing agents except black carbon on snow ($j = 9$), where an efficacy of 3 is used following Bond et al. (2013). The coefficients d_1 and d_2 govern the slow ($i = 1$) and fast ($i = 2$) temperature changes from a response to ~~radiative~~

forcing from the upper ocean and the deep ocean respectively (Millar et al., 2015). The total temperature change in year t is the sum of the slow and fast components, i.e. $T_t = T_{t,1} + T_{t,2}$. F_j represents the 13 individual forcing agents in year t calculated in section 2.2 (see also table 3). d_1 and d_2 default to 239 and 4.1 years which are fit to match the mean of CMIP5 models (Geoffroy et al., 2013). The coefficients q_1 and q_2 (units K W^{-1} m^2) are determined by solving a matrix equation given TCR, ECS, d_1, d_2 and the ERF from a doubling of CO_2, $F_{2\times} = 3.71$ W m^{-2} (Myhre et al., 2013b):

$$T_{\text{ECS}} = F_{2\times}(q_1 + q_2); \tag{22}$$

$$T_{\text{TCR}} = F_{2\times}\left(q_1\left(1 - \frac{d_1}{D}\left(1 - \exp\left(-\frac{D}{d_1}\right)\right)\right) + q_2\left(1 - \frac{d_2}{D}\left(1 - \exp\left(\frac{D}{d_2}\right)\right)\right)\right) \tag{23}$$

giving the relative contributions to the fast and slow components of the warming. $D = \log(2)/\log(1.01) \approx 69.7$ years is the time to a doubling of CO_2 with a compound 1% per year increase in CO_2 concentrations.

There is some evidence that ECS and TCR have not been constant values over the historical period (Gregory and Andrews, 2016; Gregory et al., 2015), and that ECS does not necessarily assume a constant value in CMIP5 modelling experiments (Armour, 2017). FAIR has the capability to model time-evolving ECS and TCR by updating the q_1 and q_2 values in each time step.

3 Projections using a large ensemble

To test the model response to a range of forcing pathways, we perform a 100,000-member Monte Carlo simulation using emissions from the RCP datasets (Meinshausen et al., 2011b). Emissions themselves are not altered from the RCP timeseries, but the TCR, ECS, carbon cycle response to increasing temperature (r_T) and cumulative emissions (r_C) along with theits pre-industrial value of $iIRF_{100}$ (r_0), plus the ERF scale factors for each of the 13 forcing agents, are drawn from distributions. FAIR is run from 1765 (the start of the RCP emissions datasets) to 2100.

3.1 Constraint to historical temperature observations

As a wide range of forcing, and thus temperature, scenarios can be generated, there are a proportion of ensemble members generated that fall outside the range of plausibility. We constrain the full 100,000 member ensemble (hereafter FULL) to the observed temperature change from the Cowtan and Way (2014) dataset (hereafter C&W) to assess plausibility; ensemble members that satisfy the temperature constraint are designated as Not Ruled Out Yet (NROY) and the majority of the discussion of the results in section 4 focuses on this dataset. We rebase all of the temperatures to the 1861–1880 mean following Richardson et al. (2016), to represent a "pre-industrial" state that is relatively free from volcanic eruptions but with a reasonable global coverage of temperature observations. An ordinary least-squares regression of temperature change versus time from 1880–2016 is used to calculate the linear warming trend in each ensemble member. The regression is also performed for the C&W "observational" dataset to estimate the observed warming rate. The confidence interval around the C&W warming rate is inflated by a factor that represents the lag-1 autocorrelation of residuals (i.e. the trend-line estimate from the regression minus the C&W "observations") which accounts for internal climate variability (Santer et al., 2008; Thompson et al., 2015) and is the same

method used in AR5 to estimate linear temperature trends. The constraint is satisfied for an ensemble member if the modelled trend falls within the 5–95% range of trend from C&W of 0.95 ± 0.17 K.

The C&W observed warming from 1880–2016 ~~is 0.95 ± 0.17 K,~~ higher than the HadCRUT4 estimate of 0.91 ± 0.18 K for the same timeframe ~~and the AR5 estimate of 0.85 ± 0.20 K for 1880–2012 (Hartmann et al., 2013)~~. The infilling of grid boxes where no or limited data are available accounts for these differences, as sparse observations are typically in polar regions which warm faster than the global mean (Cowtan and Way, 2014).

Under this constraint approximately 25~~26~~% of the FULL ensemble is retained in NROY.

3.2 Sampling ECS and TCR

The ECS and TCR from CMIP5 models (Forster et al., 2013) are used to generate a joint lognormal distribution. Random variables are sampled using the R package MethylCapSig[1] using the mean, standard deviation and correlation coefficient ($r = 0.81$) between ECS and TCR in CMIP5. A lognormal distribution is representative of distributions of ECS and TCR in the literature (Meinshausen et al., 2009; Rogelj et al., 2012; Flato et al., 2013; Millar et al., 2017). The sampled joint and marginal distributions are shown as black contours and curves in fig. 3.~~TCR and ECS are proposed to follow a joint lognormal distribution, based on the evaluated means and standard deviations of TCR and ECS from CMIP5 models (Flato et al., 2013; Forster et al., 2013), and representative of the distributions of ECS and TCR in the literature.~~ We sample 100,000 ECS/TCR pairs; sampled pairs where ECS $<$ TCR are rejected and redrawn. A joint distribution is used because ECS and TCR are highly correlated and low values of the realised warming fraction (TCR divided by ECS) are inconsistent with models and observations (Millar et al., 2015). For other sampled quantities in this section a 100,000 member ensemble is also generated.~~The correlation coefficient in CMIP5 models ($r = 0.81$) is used in the construction of the joint distribution.~~

3.3 Sampling thermal response and carbon cycle parameters

We allow $F_{2\times}$, the ERF due to a doubling of CO_2, to assume a Gaussian distribution with 5–95% confidence interval of 20% around the best estimate ERF of 3.71 W m^{-2} (Myhre et al., 2013b). d_1 (mean 239 years, standard deviation 63 years) and d_2 (mean 4.1 years, standard deviation 1.0 years) in eq. (21) are also varied based on truncated Gaussian distributions (no values outside $\pm 3\sigma$ allowed, primarily to prevent unrealistically small or negative values of the slow~~fast~~ response d_1~~d_2~~) ~~with mean and standard deviation equal to the CMIP5 model estimates in Geoffroy et al. (2013)~~. Although FAIR is able to model the response to time-varying ECS and TCR, we use time-invariant values in our ensemble.

Some uncertainty in the carbon cycle parameters is assumed with samples of r_0, r_C and r_T taken from Gaussian distributions. r_0, r_C and r_T are given 5–95% confidence intervals of 13% of the default parameter value following Millar et al. (2017).

[1] https://cran.r-project.org/package=MethylCapSig

3.4 Sampling ERF uncertainties

The uncertainty in each of the 13 forcing components is modelled following the 5–95% confidence intervals for each forcing from AR5 (Myhre et al., 2013b, Table 8.6) in 2011 (table 3). This is achieved by scaling the ERF values calculated in section 2.2; the uncertainty ranges are given in table 3. The scaling factor is applied to the whole time series. Most uncertainties are assumed to be Gaussian, the exceptions being contrails and BC on snow which are lognormally distributed (with geometric standard deviations 1.92 and 1.65 respectively, following AR5), and aerosols which are modelled as two half-Gaussian distributions, treating values above and below the best estimate separately. These ERF uncertainties are assumed to be uncorrelated with each other.

4 Results from the NROY ensemble for the RCP scenarios

4.1 ECS and TCR

The FULL and NROY joint and marginal distributions of ECS and TCR are shown in fig. 3.

The temperature constraint in NROY results in distributions of ECS and TCR that are lower than in FULL. Some~~Much~~ of the prior sample space in which ECS and TCR are larger than the AR5 likely ranges has been rejected in the NROY distribution. While the possibility that ECS $>$ 5 K cannot be ruled out, it appears less likely than would be inferred from CMIP5 models, although it should be stressed that time-varying feedbacks are not accounted for in this large ensemble ~~FAIR~~ which would allow ECS to increase over time (Armour, 2017). From the marginal distributions, we estimate that ECS and TCR are 2.93 (2.04 to 4.32)~~2.79 (1.97 to 4.08)~~ K and 1.59 (1.07 to 2.50)~~1.47 (1.03 to 2.23)~~ K (median; (5–95% range)) respectively in the NROY ensemble, similar to but a little more tightly constrained than the AR5 *likely* (>66% probability) ranges of 1.5 to 4.5 K and 1.0 to 2.5 K, noting that the AR5 ranges are estimated from a combination of models, observations and expert judgement. The ratio of TCR to ECS, the realised warming fraction (RWF), is approximately independent of TCR in CMIP5 models (Millar et al., 2015) and the prior distribution could alternatively be defined in terms of the TCR and RWF joint distribution, which is explored in section 5. The FULL and NROY median and 5 to 95% ranges of RWF are 0.56 (0.41 to 0.76) and 0.54 (0.41 to 0.73)~~0.53 (0.40 to 0.71)~~ respectively, which is close to~~in~~ the range of CMIP5 models (0.45 to 0.75, Millar et al. (2017)).

4.2 Historical and future greenhouse gas concentrations

The historical (1765–2005) greenhouse gas concentrations from the RCP scenarios in Meinshausen et al. (2011b) were assimilated from observations of in-situ and ice core records and represent a best estimate of the actual concentrations over this period. We therefore assume that the RCP data~~base~~ represents the best estimate of the historical concentrations and compare our estimates from the NROY ensemble using the emissions-driven model. ~~Emissions of greenhouse gases that produced these concentrations were generated from MAGICC6.~~

The FAIR model reproduces the historical concentrations of greenhouse gases (fig. 4). The atmospheric concentrations of CO_2 estimated from FAIR are up to 9 ppm lower than MAGICC6 in the period 1880~~1900~~–1950 (fig. 4a). A simple carbon

cycle model cannot reproduce the kinks in the observational CO_2 trend without large changes in the input emissions. However, between 1950 and 2005, the differences between the two curves are small. The post-2005 atmospheric CO_2 concentrations are slightly higher than those estimated by MAGICC6 for the RCP scenarios, but the MAGICC6 concentrations are within the uncertainty range from the NROY ensemble. FAIR projects best estimate CO_2 concentrations of 428 (413 to 444), 553 (528 to 581), 698 (663 to 734) and 983 (928 to 1048)~~425 (410–440), 547 (523–571), 686 (655–719) and 964 (915–1015)~~ ppm for RCP2.6, RCP4.5, RCP6 and RCP8.5 in 2100. Here, the uncertainty in CO_2 concentrations relates to the range of carbon cycle parameters and the temperature dependence on carbon uptake sampled in the large ensemble.

The historical CH_4 and N_2O concentrations in FAIR have been tuned to agree with~~be in broad agreement to~~ Meinshausen et al. (2011b) by adjusting natural emissions as described previously (fig. 4b,c). There are some small differences in the future CH_4 and N_2O concentrations in the RCPs using ~~a~~ fixed atmospheric~~methane~~ lifetimes and constant (present-day) natural emissions~~, but future N_2O concentration projections are very similar to Meinshausen et al (2011b)~~.

Kyoto Protocol gases have been grouped as HFC134a-eq based on their radiative efficiency, and ODSs grouped as CFC12-eq similarly (fig. 4d,e). Small differences between the models in future scenarios may be a result of the assumption of a change in the rate of the Brewer-Dobson circulation in MAGICC6 (Meinshausen et al., 2011a), which increases the efficiency of the stratospheric sink for these gases. This temperature-dependent effect is not included in FAIR. Over the historical period, the differences are a result of the natural emissions of CF_4 (contributing to HFC134a-eq), and CH_3Br and CH_3Cl (contributing to CFC12-eq) providing a non-zero background state of these greenhouse gas equivalents in FAIR. In the RCP historical dataset these background concentrations have not been added to the HFC134a-eq and CFC12-eq timeseries.

4.3 Historical, present and future radiative forcing

Figure 5 shows the comparison between FAIR and MAGICC6 for the 13 forcing agents considered in FAIR for the NROY ensemble. The ERF time series for the historical period in AR5 is also shown (IPCC, 2013). The updated radiative forcing relationship for CH_4 increases radiative forcing substantially (fig. 5b). The new relationship for N_2O results in a slightly lower ERF estimate in FAIR than RF in MAGICC6 (fig. 5c) which is offset by the higher concentrations of N_2O in FAIR. The FAIR estimate of CO_2 forcing is also higher than MAGICC for the RCPs, but the ERFs from FAIR and RFs from MAGICC for ~~CO_2 and~~ the minor greenhouse gases are similar (fig. 5a,d). For non-CO_2 gases, AR5 did not provide a breakdown of ERF by individual gas, so the total ERF has been scaled by the ratios in the MAGICC6 timeseries.

For tropospheric ozone, the Stevenson et al. (2013) relationship agrees well with AR5 until around 1970, from which point it is larger than AR5. There is also a large relative difference between this relationship and the MAGICC estimate in AR5 out to 2100~~the multi-linear regression method based on precursor emissions very closely emulates the AR5 ERF time series and produces sensible, albeit low-biased future ERF estimates compared to MAGICC6~~ (fig. 5e). The shape of the stratospheric ozone ERF curve between AR5 and MAGICC6 differs, but it can be seen that the AR5 historical ERF is well emulated as it uses the same functional relationship as AR5 (fig. 5f). Stratospheric water vapour from methane oxidation depends on the underlying methane forcing and is similar to~~shows the same shape as the CH_4 forcing curve but with better agreement to the MAGICC6 timeseries than~~ the AR5 timeseries (fig. 5g). Contrail ERF shows a similar time evolution over the historical period

to AR5 (fig. 5h). Historically, ERF from aviation contrails has been small, but may become more substantial in the future. The median aerosol ERF in FAIR is slightly more negative than in AR5 from around 1900 to 2011~~, which suggests that runs with larger negative aerosol forcing were more likely to satisfy the observed temperature constraint as the AR5 ERF time series was used to tune the emission coefficients~~ (fig. 5i) but is less negative than the RCP projections. We reiterate here that the RCPs report RF from MAGICC rather than ERF~~. The resulting median time series replicates the aerosol radiative forcing from MAGICC6 remarkably well from 1900 to the end of the historical period. In the future RCP scenarios, the best estimate of aerosol ERF in FAIR is stronger than in MAGICC6.~~

BC on snow has a smaller ERF in FAIR than the corresponding RF in MAGICC6, although the efficacy factor of 3 used in FAIR results in a similar effect on temperature between the models (fig. 5j). Estimates of future land use forcing in FAIR follow a similar shape to the Meinshausen et al. (2011b) dataset with slightly less negative best estimates to the AR5 ERF 2011 best estimate; agreement in the historical period to either MAGICC6 or AR5 is less good, but the general trajectory of forcing is correct (fig. 5k). There are substantial differences between the volcanic forcing datasets in FAIR, AR5 and the RCPs that are not easy to discern at the resolution of the plot (fig. 5l): generally, the AR5 dataset gives more negative forcing than the RCPs during volcanically active years, and also defines the absence of volcanoes as zero forcing whereas the RCP and FAIR datasets define zero to be the average of the historical period~~, meaning quiescent years have a small positive forcing~~. Solar forcing is used from the new CMIP6 dataset which is reasonably similar to the RCP time series for historical forcing but exhibits some differences in the future owing to the assumed inter-cycle variability that was not present in CMIP5 (fig. 5m).

Figure 5n shows the sum of the forcing components. The best estimate sum of ERF follows AR5 closely over the historical period, which is intentional. In the RCP future scenarios, the FAIR best estimates of ERF are higher than the corresponding RF estimates in MAGICC~~slightly higher than the MAGICC6 RF out to 2100 in RCP8.5, similar in RCPs 4.5 and 6.0, and lower in RCP 2.6~~. This is in part due to the increased CH_4, tropospheric ozone and contrail forcing in FAIR~~ for RCP8.5~~, and less~~more~~ negative total aerosol ERF for RCP2.6. The FAIR model projects 2100 ERFs (median and (5–95% credible intervals)) of 2.67 (2.12 to 3.25), 4.69 (3.89 to 5.53), 5.90 (4.86 to 6.98) and 9.42 (7.93 to 10.95)~~2.23 (1.46 to 3.03), 4.27 (3.40 to 5.18), 5.32 (4.16 to 6.53) and 8.71 (7.18 to 10.30)~~ W m^{-2} for RCP2.6, RCP4.5, RCP6.0 and RCP8.5 respectively.

4.4 Relationship between forcing components, ECS and TCR

The distribution of ERF in 2017 for aerosols, greenhouse gases and the anthropogenic total in both the FULL and the NROY ensembles assuming the RCP8.5 forcing pathway is shown in fig. 6 and table 6. The temperature constraint in NROY shifts the distribution of ERF for greenhouse gases slightly to the left but is similar to the FULL ensemble. For aerosols, the distribution of ERF in NROY is slightly narrower~~wider~~ than in FULL, with a reduction in the probability of a strong present-day aerosol forcing. The~~. The left-shifting of the aerosol and greenhouse gas ERF distributions in NROY results in a lower~~ median estimate of net anthropogenic ERF of 2.70~~(2.56~~ W m^{-2} in 2017~~)~~ for NROY is similar to the unconstrained FULL estimate of 2.73 W m^{-2}.

There are negative correlations between aerosol radiative forcing and ECS/TCR (fig. 7). A large negative aerosol forcing requires a high ECS to balance and recreate realistic observed temperatures (Forest et al., 2006). Millar et al. (2015) highlighted

the necessity of anti-correlation between TCR and aerosol forcing in observational constraints. The aerosol forcing on TCR constraint is tighter than that on ECS, evidenced by the narrower mass of points in the TCR plot (fig. 7b) compared to the ECS plot (fig. 7a). A high value for TCR (greater than 2.5 K) or ECS (greater than 5 K) is only possible with a strong negative present-day aerosol forcing (more negative than -1.0 W m^{-2}).

4.5 Observed and future temperature changes

Figure 8a shows the transient historical and RCP-projected temperature change for 1850–2100 along with the 2081–2100 median, 1σ (16–84% range) and 5–95% credible range for the NROY ensemble (fig. 8b), (c.f. Rogelj et al. (2012), Collins et al. (2013, fig. 12.8b)). For the RCP scenarios, the median NROY estimates of temperature change for 2081–2100 are 1.53~~1.32~~, 2.37~~2.12~~, 2.74~~2.38~~ and 4.03~~3.54~~ K above pre-industrial for RCPs 2.6, 4.5, 6.0 and 8.5 respectively. The median, 1σ and 5–95% ranges of total temperature change predicted from FAIR are about the same for RCP2.6 and RCP4.5 as~~lower than~~ those predicted by the emissions-driven MAGICC6 experiments which are reported in AR5 (Rogelj et al., 2012; Meinshausen et al., 2009), a little lower for RCP6, and substantially lower for RCP8.5. The RCP8.5 case is despite ~~marginally~~ higher 21st century ERF profiles in FAIR compared to RF in MAGICC. The difference of 0.5 K in the median end-of-century warming in RCP8.5 could be particularly important in policy assessments.

Differences between the models can arise from many sources. The results of Rogelj et al. (2012) are based on best estimates of the ECS/TCR and radiative forcing from the IPCC Fourth Assessment Report (AR4), whereas we guide FAIR using~~in this paper we use results from~~ AR5 forcings. Differences between this study and Rogelj et al. (2012) could be due to differences in the historical radiative forcing time series. The RF over the 1861–1880 to 2005 period, which forms the bulk of the period used to constrain the ensemble to observed temperatures, in Meinshausen et al. (2011b) is 1.72 W m^{-2} whereas the ERF differences are 1.98 W m^{-2} in AR5 and 1.96~~1.97~~ W m^{-2} in FAIR~~ (which is tuned to AR5)~~ over the same period. Therefore, ~~assuming Rogelj et al. (2012) used the Meinshausen et al. (2011b) radiative forcing time series or one based on AR4,~~ the same observed temperature change would be recreated with a smaller RF in Rogelj et al. (2012) than the corresponding ERF in FAIR, and the same future forcing in MAGICC6 would lead to a higher temperature change than in FAIR. ~~In relative terms the 2100 best estimate forcings between this study and Rogelj et al. (2012) are similar and hence the resulting future temperature predictions are lower in FAIR.~~ Other differences between the studies include a different selection of ECS and TCR priors in Meinshausen et al. (2009) and Rogelj et al. (2012) (based on AR4, but not substantially different from the CMIP5 models used in this study), a different method of constraining to observed temperatures, and different assumptions regarding the strength of future aerosol and ozone forcing~~ (as previously noted the median future aerosol forcing is stronger in FAIR than in the RCPs)~~. The sensitivity to some of these assumptions is tested in section 5.

4.6 Transient Climate Response to Emissions

There is an approximately linear relationship between cumulative CO_2 emissions and temperature, independent of the actual emissions pathway taken, providing temperature is still increasing (Allen et al., 2009; Collins et al., 2013). Using this linearity

we can diagnose the transient climate response to emissions (TCRE), defined as the change in temperature for a 1000 Gt cumulative emission of carbon.

We show both the TCRE assuming CO_2 forcing alone and the temperature change due to all forcing agents but measured against cumulative carbon emissions (fig. 9). When including the effect of non-CO_2 forcing on the total temperature change, the temperature response is substantially larger than for CO_2 forcing alone. This indicates that a smaller cumulative CO_2 emission is required to reach the same temperature change, and is a result of the total non-CO_2 forcing being positive. This same conclusion was reached in Collins et al. (2013) when assessing a suite of earth system models.

To determine the TCRE we run FAIR in CO_2-only modedue to the emissions of CO_2 alone, we adapt the method of Tachiiri et al. (2015). Firstly it is assumed that the temperature change due to CO_2 alone scales with ratio of CO_2 forcing to total forcing: $T_{CO_2} = T\frac{F_{CO_2}}{F}$. Secondly, to account for the fact that the efficiency of carbon sinks are temperature-dependent and noting that $T_{CO_2} < T$ when the non-CO_2 forcing is positive (all times except during volcanically active periods) the cumulative emissions since 1870 are reduced by a factor that takes into account this temperature difference. We measure cumulative CO_2 emissions and temperature change sinceuse 1870 here rather than 1850, as this is the date from which reliable estimates of carbon emissions start (Le Quéré et al., 2016) and is also at the centre of the 1861–1880 period used to evaluate temperature changes. For TCRE accounting purposes we therefore assume that cumulative carbon emissions E_{TCRE} are $E_{\mathrm{TCRE}} = (\sum_t E_{\mathrm{CO}_2,t}) - \frac{r_T}{r_0 + r_C C_{\mathrm{acc}} + r_T T} C_{\mathrm{acc}}(T - T_{\mathrm{CO}_2})$. The second term on the right of eq. (22) is the change in iIRF_{100} due to non-CO_2 forcing as a fraction of the total, multiplied by the accumulated uptake. This estimates the effect on cumulative carbon emissions as a result of non-CO_2 forcing by the effect of non-CO_2 warming on decreasing efficiency of carbon sinks. The reduction factor reduces the effective cumulative emissions by around 2.5% in 2100 in RCP8.5.

The NROY ensemble in FAIR shows a TCRE of 0.97 to 2.311.03 to 2.16 K for a cumulative carbon emission of 1000 Gt with a best estimate of 1.441.43 K. We diagnose TCRE based on the RCP8.5 simulation but this range is almost independent of the future RCP scenario (not shown) except for RCP2.6 towards the end of the 21st century in which emissions become negative. The TCRE range from FAIR is within the range of estimates from AR5 (0.8 to 2.5 K, Collins et al. (2013)). In the original FAIR model, TCRE was shown to be 1.3 (0.8 to 2.4) K (Millar et al., 2017). The narrowing of the credible interval between the original FAIR model and the emissions-based version is due to the results in this study being constrained to observed temperature change and the inclusion of non-CO_2 forcings. Towards higher cumulative CO_2 emissions in RCP8.5 the temperature response has a slightly concave shape. The slight (rather than moderate) downward curvature is also present in CMIP5 earth system models, as the increase in airborne fraction of CO_2 with emissions almost cancels out the logarithmic relationship between CO_2 concentration and temperature (Millar et al., 2016).

The TCRE curve can be inverted to consider the remaining carbon budget until either 1.5 K or 2 K total warming is reached (the limits imposed in the Paris Agreement). InTaking RCP8.5 as a best estimate, a total of 555565 GtC has been emitted over the period 1870–2016, which is close to the observational best estimate of 565 GtC (Le Quéré et al., 2016). Considering all forcing agents (the red curve in fig. 9), the cumulative emissions limit required to ensure peak warming remains under 1.5 K is 725 (590 to 943)790 (650–1010) GtC. To remain under 2 K of total warming, the allowable cumulative emissions are 968 (734 to 1323)1080 (840–1460) GtC. Millar et al. (2017a) recently showed that a further 200 GtC of additional emissions, without

~~mitigation of non-CO_2 forcing agents, would result in a peak warming of less than 1.5 K in 66% of CMIP5 earth system models. We estimate here that a further 225 GtC would give a 50% chance of peak temperature rise being less than 1.5 K, which is consistent with the conclusion of Millar et al. (2017a).~~

4.7 Top of atmosphere energy imbalance

The top of atmosphere energy imbalance N can be diagnosed from (Forster et al., 2013)

$$N = F - \lambda T \tag{24}$$

where λ is the climate feedback parameter and $\lambda = F_{2\times}/\text{ECS}$. In fig. 10 we compare FAIR model outputs from the NROY ensemble under RCP4.5 to observations of the earth's energy imbalance from satellites (Clouds and the Earth's Radiant Energy System; CERES) and from the array of Argo floats (Argo, 2000), which measure ocean temperature which is the largest component of the change in earth's energy budget. Both datasets are taken from Johnson et al. (2016).

For most years~~every year~~ from 2001 to 2015 the net energy balance from CERES is within the uncertainty range estimated from the FAIR NROY ensemble. The Argo estimate of N is more variable prior to 2005, after which coverage of the Argo floats saw a large increase (Johnson et al., 2016). From 2005 onwards, all Argo estimates but one fall inside the credible range of FAIR estimates. Both CERES and Argo observations from 2005 onwards are clustered towards the lower half of the credible range from FAIR, which may indicate that ECS over the 2005–2015 period could be towards the lower end of the credible range estimated from the NROY ensemble.

5 Sensitivity to prior distributions and constraints

To determine the robustness of the results of the NROY ensemble, the input assumptions were varied or the ensemble members subjected to a different constraint as described in this section. The results are summarised in tables 7 to 9.

5.1 Prior distributions of ECS and TCR

The prior distributions of ECS and TCR has a large influence on the posterior distributions attained (Pueyo, 2012). Here we test the dependence of the shape of the posterior distributions of ECS and TCR in the constrained samples on the choice of prior distributions.

As the RWF is approximately independent of TCR we use an alternative prior starting with the distributions of TCR and RWF. Noting the analysis of Collins et al. (2013), the AR5 likely range of TCR of 1.0 to 2.5 K is taken to be most probable, with values between 0.5–1.0 K and 2.5–3.5 K possible but unlikely. A trapezoidal distribution in TCR with these limits is constructed, therefore not expressing any prior judgement about the most likely value of TCR within the AR5 likely range. The RWF is sampled from a Gaussian distribution with mean 0.6 and 5–95% range of 0.45–0.75 following Millar et al. (2017), truncated to fall within the 0.2–1.0 range. These ranges are subjective choices based on evidence from CMIP5 models. The posterior distribution of ECS in particular can be sensitive to the choice of prior distribution (Frame et al., 2005; Pueyo, 2012).

Figure S2 shows the alternative prior distributions and the posteriors obtained as a result of constraining to the C&W observed temperatures.

~~The marginal distributions of both TCR and ECS take on a lognormal shape that is similar to the original NROY ensemble distribution (fig. 3), and weighted towards the lower end of the prior distributions. Under this prior distribution, the modal values of ECS and TCR are about 2.1 K and 1.25 K, although the median values are somewhat higher at 2.44 and 1.44 K, and the credible ranges are wider than in NROY (in fact, are very similar to the AR5 uncertainty ranges.~~

The best estimate and credible range of ERF is very similar to NROY with the alternative prior distributions (table 8). However the future temperature projections under the RCPs span a wider range than in NROY (table 9). This is due to the wider range of ECS and TCR admitted in the posterior distributions using this alternative prior.

5.2 ERF from a doubling of CO_2

The canonical RF value of $F_{2\times} = 3.71$ W m^{-2} may not be applicable when considering all land surface and tropospheric rapid adjustments in the definition of ERF. For CO_2 forcing rapid adjustments include cloud changes that are not driven by temperature change (Gregory and Webb, 2008) and land surface adjustments consequential to plant stomatal conductance (Doutriaux-Boucher et al., 2009). The mean ERF for a doubling of CO_2 in CMIP5 models was found to be 3.44 W m^{-2} (Forster et al., 2013). The simulation is repeated with this new lower ERF value for a doubling of CO_2, with the same uncertainty of 20%.

It is found that this lower value of $F_{2\times}$ slightly lowers~~does not substantially change~~ the best estimate and credible range of ECS~~, and~~ TCR and~~. The year 2100 estimates of~~ ERF, but the~~ are lower than NROY as the CO_2 forcing that is the major component of total forcing in most years is lower. The~~ temperature change under the RCP scenarios are higher than in NROY due to non-CO_2 forcings. This behaviour can be analysed with the help of eq. (24). In equilibrium states, the TOA energy imbalance $N = 0$ and eq. (24) is rearranged to yield $T = F_{2\times}/\lambda$. If $F_{2\times}$ is found to take a lower value, and ensemble members are constrained to the same observed temperature, then the climate sensitivity $1/\lambda$ must be higher to compensate. Therefore, the same positive future non-CO_2 forcing time series will produce higher temperatures in the future. ~~Aerosol emissions-forcing relationship There is evidence that the negative radiative forcing from aerosols begins to saturate as emissions increase (Twomey et al., 2013; Carslaw et al., 2013). In particular, Stevens (2015) used a simple model to suggest that sulfate aerosol forcing is too strong in CMIP5 models, and claims that aerosol forcing has a realistic lower bound (maximum negative) of -1.0 W m^{-2}. Subsequent analysis of the aerosol forcing and temperature change in CMIP5 models over the 1850–1950 period has questioned this conclusion (Kretzschmar et al., 2017), but we use Stevens' formulation to investigate the effects of a very different aerosol forcing scenario. The importance of the aerosol forcing relationship is tested by using the simple relationship proposed by Stevens (2015)~~

$$F_{\text{aero}} = -\alpha_S E_{\text{SO}_2} - \beta_S \log\left(\frac{E_{\text{SO}_2}}{E_{\text{SO}_2,\text{nat}}}\right)$$

~~with α_S and β_S forcing efficiencies and $E_{\text{SO}_2,\text{nat}}$ the background natural emissions of sulfate aerosol (note no dependence on the emissions of any other aerosol species). To provide a distribution of inputs we follow Stevens (2015) where $1/\alpha_S$ follows~~

~~a Gaussian distribution (mean 600, standard deviation 200 Tg SO_2 (W m^{-2})$^{-1}$) and $E_{SO_2,nat}$ is Gaussian with mean 60 and 2.5–97.5% range of 30 Tg SO_2. β_S is not perturbed from its default value of 0.634 W m^{-2} as the uncertainty in F_{aci} is captured in the variation of $E_{SO_2,nat}$. Furthermore, unlike with the linear relationship for aerosol forcing with emissions, we do not apply the AR5 uncertainty scalings to the model-derived aerosol forcing as it assumed that all of the uncertainty is captured with the variation of α_S and $E_{SO_2,nat}$. The impact of this aerosol relationship is a narrowing of the credible ranges of ECS, TCR and TCRE, although with similar best estimates to NROY. The saturation effect of the aerosol ERF means there are very few ensemble members with a large negative aerosol forcing in the present day, and as such the year 2100 ERF projections are higher than NROY for all RCPs. The increase in net forcing impacts on year 2100 temperatures, which are also higher that NROY for all except the upper bound in RCP8.5.~~

5.3 Historical temperature constraint

Historical temperatures were also constrained using the HadCRUT4 dataset without infilling (Morice et al., 2012), along with the GISTEMP (Hansen et al., 2010), Berkeley Earth (Berkeley Earth, 2017) and NOAA (Zhang et al., 2017) observational datasets. The linear 1880–2016 trends are 0.91 ± 0.18 K, 0.99 ± 0.22 K, 1.07 ± 0.16 K and 0.93 ± 0.24 K respectively. All datasets, including C&W (0.95 ± 0.17 K), were accessed on 17 October 2017.

We also perform analysis on the FULL dataset, where the input assumptions are guided by CMIP5 models and AR5 uncertainty ranges but no constraint to historical temperature is performed. We show in tables 7 to 9 that ECS, TCR, TCRE, ERF and temperature change depend slightly on the dataset of constraint, with datasets showing more warming over the historical period also projecting warmer 2100 temperatures under the RCP scenarios. Using the FULL ensemble however leads to wide uncertainty bounds and higher median estimates of these diagnosed parameters than using any of the constrained ensembles. Therefore, using a historical temperature constraint rejects parameter combinations that produce larger future temperature changes.

6 Conclusions

We present a simple model, FAIR v1.2~~1~~, that calculates global temperature change, effective radiative forcing from a variety of drivers, and concentrations of greenhouse gases. The emissions-based model is based on the FAIR v1.0 carbon cycle-climate model with an extension for emissions of non-CO_2 greenhouse gases, ozone precursors and aerosols. This version of FAIR, which is tuned to the effective radiative forcing timeseries in AR5 over the historical period, provides ERFs that are ~~is~~ close to the target radiative forcings from the RCP scenarios in 2100. FAIR was not tuned to emulate the radiative forcing in the MAGICC6 model, however it ~~reproduces the trends in future radiative forcing from the RCPs in MAGICC6 and~~ closely matches the concentrations of greenhouse gases projected in that model.

Within FAIR, the response of the carbon cycle model can be adjusted via the rate of uptake of carbon by land and ocean processes parameterised as a function of total temperature change and cumulative carbon emissions ($iIRF_{100}$). Emissions and concentrations are converted to effective radiative forcing and the relationship of ERF to temperature change is governed by

the TCR, ECS, and the efficacy of each of the 13 separate forcing categories considered in the model. The emulation~~replication~~ of specific earth system models is therefore possible as discussed by Millar et al. (2017).

Using a correlated joint lognormal prior distribution of ECS and TCR based on CMIP5 models, running a 100,000 member ensemble in FAIR and keeping only those ensemble members that match the rate of temperature change from 1880–2016 in from Cowtan & Way (the not ruled out yet or NROY ensemble), we find that the median and 5–95% credible range of ECS and TCR to be 2.93 (2.04 to 4.32)~~2.79 (1.97 to 4.08)~~ K and 1.58 (1.07 to 2.50)~~1.47 (1.03 to 2.23)~~ K respectively. The transient climate response to CO_2 emissions (TCRE) is diagnosed from a CO_2-only~~a diagnostic output from the NROY~~ ensemble and found to be 1.44 (0.97 to 2.31)~~1.43 (1.01 to 2.16)~~ K $(1000\ \mathrm{GtC})^{-1}$. These ranges are similar to the IPCC AR5 likely ranges for ECS, TCR and TCRE, albeit with tighter credible bounds~~ and shifted slightly towards the low end of the ranges~~. The NROY best estimates and ranges are not very~~mildly~~ sensitive to a lower estimate of the ERF from a doubling of CO_2 or a different observational temperature datasets to constrain the historical temperature change rather than the Cowtan and Way (2014) dataset. They are more sensitive to the prior distribution of ECS and TCR, particularly for the constraint on ECS. ~~They are also mildly sensitive to a non-linear aerosol forcing assumption or using a different prior ECS/TCR distribution, although the former may overconstrain ECS and TCR.~~ All methods of constraint lead to lower median and credible range estimates of ECS, TCR and TCRE than not constraining to temperature at all (the FULL ensemble, with input parameters estimated from the distribution of CMIP5 models and ERF uncertainties based on AR5 estimates).

Our estimate of TCR is not as low as the range derived by Otto et al. (2013) from observational constraints (0.9 to 2.0 K)~~, although they used HadCRUT4 to constrain with the lower value of doubled-CO_2 ERF with a simpler regression-based model of ERF to temperature change~~. Similarly our best estimate of ECS is higher than the estimate provided by Gregory and Andrews (2016) of around 2 K using observed sea-surface temperatures and sea-ice in two atmosphere-only GCMs. While we cannot absolutely rule out values of ECS greater than 5 K or TCR greater than 2.5 K, this would require a strong present-day aerosol forcing (at least as negative as $-1.0\ \mathrm{W\ m^{-2}}$, but probably more so) to balance. Progress towards tightening these upper bounds could therefore be achieved with a better understanding of the present-day aerosol forcing (Stevens et al., 2016).

Temperature changes projected in the NROY ensemble in 2100 are similar to~~lower than~~ those from Rogelj et al. (2012) for the RCP scenarios, except for RCP8.5 where the FAIR is 0.5 K lower in the median response. This is due to the lower ensemble estimates of ECS and TCR in NROY, and the differences in present-day minus 1850 radiative forcing between AR5/NROY and the RCP radiative forcing in Meinshausen et al. (2011b). Nevertheless, under RCP8.5 the median year 2100 temperature projection is 4.45~~3.94~~ K above the pre-industrial in our NROY ensemble, which would have very severe global consequences. Conversely the median estimate for RCP2.6 is 1.52~~1.34~~ K, suggesting about a ~~greater than~~ 50% chance of limiting end-of-century warming to 1.5 K under this pathway.

FAIR~~The emissions-based FAIR model~~ is useful for creating large ensembles of future temperature change based on input uncertainties in the carbon cycle parameters and effective radiative forcing strengths. This can be used for instance to assess the impacts of emissions commitment scenarios or committed warming (Ehlert and Zickfeld, 2017), or if a certain category of emissions such as aerosols are increased or decreased in the future. FAIR can be used with integrated assessment models to calculate the social cost of carbon in the presence of non-CO_2 forcing agents. Following the 2015 Paris Agreement and in

anticipation of the 2018 IPCC Special Report, the FAIR model can be used to investigate emissions pathways consistent with 1.5 K and 2 K total warming limits, including remaining carbon budgets, and give probabilistic indications of the likelihood of these limits being breached.

Code availability. The source code can be obtained at https://github.com/OMS-NetZero/FAIR and can also be installed from the Python Package Index (https://pypi.org/project/fair/). A user guide is included in the supplementary material.

Competing interests. The authors declare that they have no conflict of interest.

Acknowledgements. CJS and PMF acknowledge financial support from the Natural Environment Research Council under grant NE/N006038/1. The authors are grateful to Zebedee Nicholls and Robert Gieseke for assistance with repository management and code streamlining.

References

Albrecht, B. A.: Aerosols, cloud microphysics, and fractional cloudiness, Science, 245, 1227–1231, 1989.

Allen, M. R., Frame, D. J., Huntingford, C., Jones, C. D., Lowe, J. A., Meinshausen, M., and Meinshausen, N.: Warming caused by cumulative carbon emissions towards the trillionth tonne, Nature, 458, 1163–1166, https://doi.org/10.1038/nature08019, 2009.

Andrews, T., Betts, R. A., Booth, B. B. B., Jones, C. D., and Jones, G. S.: Effective radiative forcing from historical land use change, Clim. Dynam., 48, 3489–3505, https://doi.org/10.1007/s00382-016-3280-7, 2017.

Argo: Argo float data and metadata from Global Data Assembly Centre (Argo GDAC). SEANOE, https://doi.org/10.17882/42182, 2000.

Armour, K.: Energy budget constraints on climate sensitivity in light of inconstant climate feedbacks, Nat. Clim. Change, 7, 331–335, https://doi.org/10.1038/nclimate3278, 2017.

Berkeley Earth: Land + Ocean (1850 - Recent) Monthly Global Average Temperature, http://berkeleyearth.lbl.gov/auto/Global/Land_and_Ocean_complete.txt, accessed 17 October 2017, 2017.

Bond, T. C., Doherty, S. J., Fahey, D. W., Forster, P. M., Berntsen, T., DeAngelo, B. J., Flanner, M. G., Ghan, S., Kärcher, B., Koch, D., Kinne, S., Kondo, Y., Quinn, P. K., Sarofim, M. C., Schultz, M. G., Schulz, M., Venkataraman, C., Zhang, H., Zhang, S., Bellouin, N., Guttikunda, S. K., Hopke, P. K., Jacobson, M. Z., Kaiser, J. W., Klimont, Z., Lohmann, U., Schwarz, J. P., Shindell, D., Storelvmo, T., Warren, S. G., and Zender, C. S.: Bounding the role of black carbon in the climate system: A scientific assessment, J. Geophys. Res.-Atmos., 118, 5380–5552, https://doi.org/10.1002/jgrd.50171, 2013.

Boucher, O. and Reddy, M.: Climate trade-off between black carbon and carbon dioxide emissions, Energ. Policy, 36, 193–200, https://doi.org/10.1016/j.enpol.2007.08.039, 2008.

Boucher, O., Friedlingstein, P., Collins, B., and Shine, K. P.: The indirect global warming potential and global temperature change potential due to methane oxidation, Environ. Res. Lett., 4, 044 007, https://doi.org/10.1088/1748-9326/4/4/044007, 2009.

Boucher, O., Randall, D., Artaxo, P., Bretherton, C., Feingold, G., Forster, P., Kerminen, V.-M., Kondo, Y., Liao, H., Lohmann, U., Rasch, P., Satheesh, S., Sherwood, S., Stevens, B., and Zhang, X.: Clouds and Aerosols, in: Climate Change 2013: The Physical Science Basis. Contribution of Working Group I to the Fifth Assessment Report of the Intergovernmental Panel on Climate Change, edited by Stocker, T., Qin, D., Plattner, G.-K., Tignor, M., Allen, S., Boschung, J., Nauels, A., Xia, Y., Bex, V., and Midgley, P., pp. 571–658, Cambridge University Press, Cambridge, United Kingdom and New York, NY, USA, 2013.

Carslaw, K., Lee, L., Reddington, C., Pringle, K., Rap, A., Forster, P., Mann, G., Spracklen, D., Woodhouse, M., Regayre, L., and Pierce, J.: Large contribution of natural aerosols to uncertainty in indirect forcing, Nature, 503, 67, https://doi.org/10.1038/nature12674, 2013.

Collins, M., Knutti, R., Arblaster, J., Dufresne, J.-L., Fichefet, T., Friedlingstein, P., Gao, X., Gutowski, W., Johns, T., Krinner, G., Shongwe, M., Tebaldi, C., Weaver, A., and Wehner, M.: Long-term Climate Change: Projections, Commitments and Irreversibility, in: Climate Change 2013: The Physical Science Basis. Contribution of Working Group I to the Fifth Assessment Report of the Intergovernmental Panel on Climate Change, edited by Stocker, T., Qin, D., Plattner, G.-K., Tignor, M., Allen, S., Boschung, J., Nauels, A., Xia, Y., Bex, V., and Midgley, P., pp. 1029–1136, Cambridge University Press, Cambridge, United Kingdom and New York, NY, USA, https://doi.org/10.1017/CBO9781107415324.024, 2013.

Cowtan, K. and Way, R. G.: Coverage bias in the HadCRUT4 temperature series and its impact on recent temperature trends, Q. J. Roy. Meteor. Soc., 140, 1935–1944, https://doi.org/10.1002/qj.2297, 2014.

Daniel, J. and Velders, G.: A focus on information and options for policymakers, in: Scientific Assessment of Ozone Depletion, edited by Ennis, C. A., p. 516, World Meteorological Organization, Geneva, Switzerland, 2011.

Daniel, J. S. and Solomon, S.: On the climate forcing of carbon monoxide, J. Geophys. Res.-Atmos., 103, 13 249–13 260, https://doi.org/10.1029/98JD00822, 1998.

Daniel, J. S., Solomon, S., Portmann, R. W., and Garcia, R. R.: Stratospheric ozone destruction: The importance of bromine relative to chlorine, J. Geophys. Res.-Atmos., 104, 23 871–23 880, https://doi.org/10.1029/1999JD900381, 1999.

Doutriaux-Boucher, M., Webb, M. J., Gregory, J. M., and Boucher, O.: Carbon dioxide induced stomatal closure increases radiative forcing via a rapid reduction in low cloud, Geophys. Res. Lett., 36, https://doi.org/10.1029/2008GL036273, l02703, 2009.

Ehlert, D. and Zickfeld, K.: What determines the warming commitment after cessation of CO_2 emissions?, Environ. Res. Lett., 12, 015 002, https://doi.org/10.1088/1748-9326/aa564a, 2017.

Etminan, M., Myhre, G., Highwood, E. J., and Shine, K. P.: Radiative forcing of carbon dioxide, methane, and nitrous oxide: A significant revision of the methane radiative forcing, Geophys. Res. Lett., 43, 12,614–12,623, https://doi.org/10.1002/2016GL071930, 2016GL071930, 2016.

Flato, G., Marotzke, J., Abiodun, B., Braconnot, P., Chou, S., Collins, W., Cox, P., Driouech, F., Emori, S., Eyring, V., Forest, C., Gleckler, P., Guilyardi, E., Jakob, C., Kattsov, V., Reason, C., and Rummukainen, M.: Evaluation of Climate Models, in: Climate Change 2013: The Physical Science Basis. Contribution of Working Group I to the Fifth Assessment Report of the Intergovernmental Panel on Climate Change, edited by Stocker, T., Qin, D., Plattner, G.-K., Tignor, M., Allen, S., Boschung, J., Nauels, A., Xia, Y., Bex, V., and Midgley, P., pp. 741–866, Cambridge University Press, Cambridge, United Kingdom and New York, NY, USA, 2013.

Forest, C. E., Stone, P. H., and Sokolov, A. P.: Estimated PDFs of climate system properties including natural and anthropogenic forcings, Geophys. Res. Lett., 33, https://doi.org/10.1029/2005GL023977, l01705, 2006.

Forster, P., Richardson, T., Maycock, A., Smith, C., Samset, B., Myhre, G., Andrews, T., Pincus, R., and Schulz, M.: Recommendations for diagnosing effective radiative forcing from climate models from CMIP6, J. Geophys. Res., 121, 12 460–12 475, https://doi.org/10.1002/2016JD025320, 2016.

Forster, P. M., Andrews, T., Good, P., Gregory, J. M., Jackson, L. S., and Zelinka, M.: Evaluating adjusted forcing and model spread for historical and future scenarios in the CMIP5 generation of climate models, J. Geophys. Res.-Atmos., 118, 1139–1150, https://doi.org/10.1002/jgrd.50174, 2013.

Frame, D. J., Booth, B. B. B., Kettleborough, J. A., Stainforth, D. A., Gregory, J. M., Collins, M., and Allen, M. R.: Constraining climate forecasts: The role of prior assumptions, Geophys. Res. Lett., 32, https://doi.org/10.1029/2004GL022241, l09702, 2005.

Friedlingstein, P.: Carbon cycle feedbacks and future climate change, Philos. T. R. Soc. A., 373, https://doi.org/10.1098/rsta.2014.0421, 2015.

Friedlingstein, P., Cox, P., Betts, R., Bopp, L., von Bloh, W., Brovkin, V., Cadule, P., Doney, S., Eby, M., Fung, I., Bala, G., John, J., Jones, C., Joos, F., Kato, T., Kawamiya, M., Knorr, W., Lindsay, K., Matthews, H. D., Raddatz, T., Rayner, P., Reick, C., Roeckner, E., Schnitzler, K.-G., Schnur, R., Strassmann, K., Weaver, A. J., Yoshikawa, C., and Zeng, N.: Climate–Carbon Cycle Feedback Analysis: Results from the C4MIP Model Intercomparison, J. Climate, 19, 3337–3353, https://doi.org/10.1175/JCLI3800.1, 2006.

Fung, I. Y., Doney, S. C., Lindsay, K., and John, J.: Evolution of carbon sinks in a changing climate, P. Natl. Acad. Sci. USA, 102, 11 201–11 206, https://doi.org/10.1073/pnas.0504949102, 2005.

Geoffroy, O., Saint-Martin, D., Olivié, D. J. L., Voldoire, A., Bellon, G., and Tytéca, S.: Transient Climate Response in a Two-Layer Energy-Balance Model. Part I: Analytical Solution and Parameter Calibration Using CMIP5 AOGCM Experiments, J. Climate, 26, 1841–1857, https://doi.org/10.1175/JCLI-D-12-00195.1, 2013.

Ghan, S. J., Smith, S. J., Wang, M., Zhang, K., Pringle, K., Carslaw, K., Pierce, J., Bauer, S., and Adams, P.: A simple model of global aerosol indirect effects, J. Geophys. Res.-Atmos., 118, 6688–6707, https://doi.org/10.1002/jgrd.50567, 2013.

Gillenwater, M.: Forgotten carbon: indirect CO_2 in greenhouse gas emission inventories, Environ. Sci. Policy, 11, 195–203, https://doi.org/10.1016/j.envsci.2007.09.001, 2008.

Good, P., Gregory, J. M., and Lowe, J. A.: A step-response simple climate model to reconstruct and interpret AOGCM projections, Geophys. Res. Lett., 38, https://doi.org/10.1029/2010GL045208, l01703, 2011.

Good, P., Gregory, J. M., Lowe, J. A., and Andrews, T.: Abrupt CO2 experiments as tools for predicting and understanding CMIP5 representative concentration pathway projections, Clim. Dynam., 40, 1041–1053, https://doi.org/10.1007/s00382-012-1410-4, 2013.

Gregory, J. and Webb, M.: Tropospheric adjustment induces a cloud component in CO_2 forcing, J. Climate, 21, 58–71, https://doi.org/10.1175/2007JCLI1834.1, 2008.

Gregory, J. M. and Andrews, T.: Variation in climate sensitivity and feedback parameters during the historical period, Geophys. Res. Lett., 43, 3911–3920, https://doi.org/10.1002/2016GL068406, 2016GL068406, 2016.

Gregory, J. M., Andrews, T., and Good, P.: The inconstancy of the transient climate response parameter under increasing CO2, Philos. T. R. Soc. A, 373, https://doi.org/10.1098/rsta.2014.0417, 2015.

Gregory, J. M., Andrews, T., Good, P., Mauritsen, T., and Forster, P. M.: Small global-mean cooling due to volcanic radiative forcing, Clim. Dynam., 47, 3979–3991, https://doi.org/10.1007/s00382-016-3055-1, 2016.

Hansen, J., Ruedy, R., Sato, M., and Lo, K.: Global surface temperature change, Rev. Geophys., 48, RG4004, https://doi.org/10.1029/2010RG000345, accessed 17 October 2017, 2010.

Holmes, C. D., Prather, M. J., Søvde, O. A., and Myhre, G.: Future methane, hydroxyl, and their uncertainties: key climate and emission parameters for future predictions, Atmos. Chem. Phys., 13, 285–302, https://doi.org/10.5194/acp-13-285-2013, 2013.

IPCC: Annex II: Climate System Scenario Tables, in: Climate Change 2013: The Physical Science Basis. Contribution of Working Group I to the Fifth Assessment Report of the Intergovernmental Panel on Climate Change [Stocker, T.F., D. Qin, G.-K. Plattner, M. Tignor, S.K. Allen, J. Boschung, A. Nauels, Y. Xia, V. Bex and P.M. Midgley (eds.)], edited by Prather, M., Flato, G., Friedlingstein, P., Jones, C., Lamarque, J.-F., Liao, H., and Rasch, P., Cambridge University Press, Cambridge, United Kingdom and New York, NY, USA, 2013.

Johnson, G., Lyman, J., and Loeb, N.: Improving estimates of Earth's energy imbalance, Nat. Clim. Change, 6, 639–640, https://doi.org/10.1038/nclimate3043, 2016.

Jones, A. D., Calvin, K. V., Collins, W. D., and Edmonds, J.: Accounting for radiative forcing from albedo change in future global land-use scenarios, Climatic Change, 131, 691–703, https://doi.org/10.1007/s10584-015-1411-5, 2015.

Joos, F., Roth, R., Fuglestvedt, J., Peters, G., Enting, I., von Bloh, W., Brovkin, V., Burke, E., Eby, M., Edwards, N., Friedrich, T., Frölicher, T. L., Halloran, P. R., Holden, P. B., Jones, C., Kleinen, T., Mackenzie, F. T., Matsumoto, K., Meinshausen, M., Plattner, G.-K., Reisinger, A., Segschneider, J., Shaffer, G., Steinacher, M., Strassmann, K., Tanaka, K., Timmermann, A., and Weaver, A. J.: Carbon dioxide and climate impulse response functions for the computation of greenhouse gas metrics: a multi-model analysis, Atmos. Chem. Phys., 13, 2793–2825, 2013.

Kristiansen, N. I., Stohl, A., Olivié, D. J. L., Croft, B., Søvde, O. A., Klein, H., Christoudias, T., Kunkel, D., Leadbetter, S. J., Lee, Y. H., Zhang, K., Tsigaridis, K., Bergman, T., Evangeliou, N., Wang, H., Ma, P.-L., Easter, R. C., Rasch, P. J., Liu, X., Pitari, G., Di Genova, G., Zhao, S. Y., Balkanski, Y., Bauer, S. E., Faluvegi, G. S., Kokkola, H., Martin, R. V., Pierce, J. R., Schulz, M., Shindell, D., Tost, H., and Zhang, H.: Evaluation of observed and modelled aerosol lifetimes using radioactive tracers of opportunity and an ensemble of 19 global models, Atmos. Chem. Phys., 16, 3525–3561, https://doi.org/10.5194/acp-16-3525-2016, 2016.

Lamarque, J.-F., Bond, T. C., Eyring, V., Granier, C., Heil, A., Klimont, Z., Lee, D., Liousse, C., Mieville, A., Owen, B., Schultz, M. G., Shindell, D., Smith, S. J., Stehfest, E., Van Aardenne, J., Cooper, O. R., Kainuma, M., Mahowald, N., McConnell, J. R., Naik, V., Riahi, K., and van Vuuren, D. P.: Historical (1850–2000) gridded anthropogenic and biomass burning emissions of reactive gases and aerosols: methodology and application, Atmos. Chem. and Phys., 10, 7017–7039, https://doi.org/10.5194/acp-10-7017-2010, https://www.atmos-chem-phys.net/10/7017/2010/, 2010.

Le Quéré, C., Andrew, R. M., Canadell, J. G., Sitch, S., Korsbakken, J. I., Peters, G. P., Manning, A. C., Boden, T. A., Tans, P. P., Houghton, R. A., Keeling, R. F., Alin, S., Andrews, O. D., Anthoni, P., Barbero, L., Bopp, L., Chevallier, F., Chini, L. P., Ciais, P., Currie, K., Delire, C., Doney, S. C., Friedlingstein, P., Gkritzalis, T., Harris, I., Hauck, J., Haverd, V., Hoppema, M., Klein Goldewijk, K., Jain, A. K., Kato, E., Körtzinger, A., Landschützer, P., Lefèvre, N., Lenton, A., Lienert, S., Lombardozzi, D., Melton, J. R., Metzl, N., Millero, F., Monteiro, P. M. S., Munro, D. R., Nabel, J. E. M. S., Nakaoka, S.-I., O'Brien, K., Olsen, A., Omar, A. M., Ono, T., Pierrot, D., Poulter, B., Rödenbeck, C., Salisbury, J., Schuster, U., Schwinger, J., Séférian, R., Skjelvan, I., Stocker, B. D., Sutton, A. J., Takahashi, T., Tian, H., Tilbrook, B., van der Laan-Luijkx, I. T., van der Werf, G. R., Viovy, N., Walker, A. P., Wiltshire, A. J., and Zaehle, S.: Global Carbon Budget 2016, Earth Syst. Sci. Data, 8, 605–649, https://doi.org/10.5194/essd-8-605-2016, 2016.

Lee, D. S., Fahey, D. W., Forster, P. M., Newton, P. J., Wit, R. C., Lim, L. L., Owen, B., and Sausen, R.: Aviation and global climate change in the 21st century, Atmos. Environ., 43, 3520–3537, https://doi.org/10.1016/j.atmosenv.2009.04.024, 2009.

MacDougall, A. H., Zickfeld, K., Knutti, R., and Matthews, H. D.: Sensitivity of carbon budgets to permafrost carbon feedbacks and non-CO 2 forcings, Environ. Res. Lett., 10, 125 003, https://doi.org/10.1088/1748-9326/11/1/019501, 2015.

Matthes, K., Funke, B., Andersson, M. E., Barnard, L., Beer, J., Charbonneau, P., Clilverd, M. A., Dudok de Wit, T., Haberreiter, M., Hendry, A., Jackman, C. H., Kretzschmar, M., Kruschke, T., Kunze, M., Langematz, U., Marsh, D. R., Maycock, A. C., Misios, S., Rodger, C. J., Scaife, A. A., Seppälä, A., Shangguan, M., Sinnhuber, M., Tourpali, K., Usoskin, I., van de Kamp, M., Verronen, P. T., and Versick, S.: Solar forcing for CMIP6 (v3.2), Geosci. Model Dev., 10, 2247–2302, https://doi.org/10.5194/gmd-10-2247-2017, 2017.

Matthews, H. and Zickfeld, K.: Climate response to zeroed emissions of greenhouse gases and aerosols, Nat. Clim. Change, 2, 338–341, https://doi.org/10.1038/nclimate1424, 2012.

Meinshausen, M., Meinshausen, N., Hare, W., Raper, S. C., Frieler, K., Knutti, R., Frame, D. J., and Allen, M. R.: Greenhouse-gas emission targets for limiting global warming to 2 C, Nature, 458, 1158–1162, 2009.

Meinshausen, M., Raper, S., and Wigley, T.: Emulating coupled atmosphere-ocean and carbon cycle models with a simpler model, MAGICC6 – Part 1: Model description and calibration, Atmos. Chem. Phys., 11, 1417–1456, https://doi.org/10.5194/acp-11-1417-2011, 2011a.

Meinshausen, M., Smith, S., Calvin, K., Daniel, J., Kainuma, M., Lamarque, J.-F., Matsumoto, K., Montzka, S., Raper, S., Riahi, K., Thomson, A., Velders, G., and van Vuuren, D.: The RCP Greenhouse Gas Concentrations and their Extension from 1765 to 2300, Climatic Change, https://doi.org/10.1007/s10584-011-0156-z, 2011b.

Millar, R., Allen, M., Rogelj, J., and Friedlingstein, P.: The cumulative carbon budget and its implications, Oxford Rev. Econ. Pol, 32, 323–342, https://doi.org/10.1093/oxrep/grw009, 2016.

Millar, R. J., Otto, A., Forster, P. M., Lowe, J. A., Ingram, W. J., and Allen, M. R.: Model structure in observational constraints on transient climate response, Climatic Change, 131, 199–211, https://doi.org/10.1007/s10584-015-1384-4, 2015.

Millar, R. J., Nicholls, Z. R., Friedlingstein, P., and Allen, M. R.: A modified impulse-response representation of the global near-surface air temperature and atmospheric concentration response to carbon dioxide emissions, Atmos. Chem. Phys., 2017, 7213–7228, https://doi.org/10.5194/acp-17-7213-2017, 2017.

Morice, C. P., Kennedy, J. J., Rayner, N. A., and Jones, P. D.: Quantifying uncertainties in global and regional temperature change using an ensemble of observational estimates: The HadCRUT4 dataset, J. Geophys. Res., 117, D08 101, https://doi.org/10.1029/2011JD017187, accessed 17 October 2017, 2012.

Moss, R. H., Edmonds, J. A., Hibbard, K. A., Manning, M. R., Rose, S. K., Vuuren, D. P. v., Carter, T. R., Emori, S., Kainuma, M., Kram, T., Meehl, G. A., Mitchell, J. F. B., Nakicenovic, N., Riahi, K., Smith, S. J., Stouffer, R. J., Thomson, A. M., Weyant, J. P., and Wilbanks, T. J.: The next generation of scenarios for climate change research and assessment, Nature, 463, 747–756, https://doi.org/10.1038/nature08823, 2010.

Myhre, G. and Myhre, A.: Uncertainties in Radiative Forcing due to Surface Albedo Changes Caused by Land-Use Changes, J. Climate, 16, 1511–1524, https://doi.org/10.1175/1520-0442-16.10.1511, 2003.

Myhre, G., Highwood, E. J., Shine, K. P., and Stordal, F.: New estimates of radiative forcing due to well mixed greenhouse gases, Geophys. Res. Lett., 25, 2715–2718, https://doi.org/10.1029/98GL01908, 1998.

Myhre, G., Samset, B. H., Schulz, M., Balkanski, Y., Bauer, S., Berntsen, T. K., Bian, H., Bellouin, N., Chin, M., Diehl, T., Easter, R. C., Feichter, J., Ghan, S. J., Hauglustaine, D., Iversen, T., Kinne, S., Kirkevåg, A., Lamarque, J.-F., Lin, G., Liu, X., Lund, M. T., Luo, G., Ma, X., van Noije, T., Penner, J. E., Rasch, P. J., Ruiz, A., Seland, Ø., Skeie, R. B., Stier, P., Takemura, T., Tsigaridis, K., Wang, P., Wang, Z., Xu, L., Yu, H., Yu, F., Yoon, J.-H., Zhang, K., Zhang, H., and Zhou, C.: Radiative forcing of the direct aerosol effect from AeroCom Phase II simulations, Atmos. Chem. Phys., 13, 1853–1877, https://doi.org/10.5194/acp-13-1853-2013, http://www.atmos-chem-phys.net/13/1853/2013/, 2013a.

Myhre, G., Shindell, D., Bréon, F.-M., Collins, W., Fuglestvedt, J., Huang, J., Koch, D., Lamarque, J.-F., Lee, D., Mendoza, B., Nakajima, T., Robock, A., Stephens, G., Takemura, T., and Zhang, H.: Anthropogenic and Natural Radiative Forcing, in: Climate Change 2013: The Physical Science Basis. Contribution of Working Group I to the Fifth Assessment Report of the Intergovernmental Panel on Climate Change, edited by Stocker, T., Qin, D., Plattner, G.-K., Tignor, M., Allen, S., Boschung, J., Nauels, A., Xia, Y., Bex, V., and Midgley, P., pp. 659–740, Cambridge University Press, Cambridge, United Kingdom and New York, NY, USA, 2013b.

Newman, P. A., Daniel, J. S., Waugh, D. W., and Nash, E. R.: A new formulation of equivalent effective stratospheric chlorine (EESC), Atmos. Chem. Phys., 7, 4537–4552, https://doi.org/10.5194/acp-7-4537-2007, https://www.atmos-chem-phys.net/7/4537/2007/, 2007.

Otto, A., Otto, F. E. L., Boucher, O., Church, J., Hegerl, G., Forster, P. M., Gillett, N. P., Gregory, J., Johnson, G. C., Knutti, R., Lewis, N., Lohmann, U., Marotzke, J., Myhre, G., Shindell, D., Stevens, B., and Allen, M. R.: Energy budget constraints on climate response, Nat. Geosci., 6, 415–416, https://doi.org/10.1038/ngeo1836, 2013.

Pielke, R. A., Marland, G., Betts, R. A., Chase, T. N., Eastman, J. L., Niles, J. O., Niyogi, D. D. S., and Running, S. W.: The Influence of Land-Use Change and Landscape Dynamics on the Climate System: Relevance to Climate-Change Policy beyond the Radiative Effect of Greenhouse Gases, Philos. T. R. Soc. A, 360, 1705–1719, 2002.

Prather, M. J., Holmes, C. D., and Hsu, J.: Reactive greenhouse gas scenarios: Systematic exploration of uncertainties and the role of atmospheric chemistry, Geophys. Res. Lett., 39, https://doi.org/10.1029/2012GL051440, l09803, 2012.

Pueyo, S.: Solution to the paradox of climate sensitivity, Climatic change, 113, 163–179, https://doi.org/10.1007/s10584-011-0328-x, 2012.

RCP Database: RCP Database version 2.0 hosted at IIASA, http://www.iiasa.ac.at/web-apps/tnt/RcpDb. Accessed 27/07/2017, 2009.

Richardson, M., Cowtan, K., Hawkins, E., and Stolpe, M. B.: Reconciled climate response estimates from climate models and the energy budget of Earth, Nat. Clim. Change, 2016.

Rogelj, J., Meinshausen, M., and Knutti, R.: Global warming under old and new scenarios using IPCC climate sensitivity range estimates, Nat. Clim. Change, 2, 248–253, https://doi.org/10.1038/nclimate1385, 2012.

Santer, B. D., Thorne, P. W., Haimberger, L., Taylor, K. E., Wigley, T. M. L., Lanzante, J. R., Solomon, S., Free, M., Gleckler, P. J., Jones, P. D., Karl, T. R., Klein, S. A., Mears, C., Nychka, D., Schmidt, G. A., Sherwood, S. C., and Wentz, F. J.: Consistency of modelled and observed temperature trends in the tropical troposphere, Int. J. Climatol., 28, 1703–1722, https://doi.org/10.1002/joc.1756, http://dx.doi.org/10.1002/joc.1756, 2008.

Shindell, D. T., Faluvegi, G., Koch, D. M., Schmidt, G. A., Unger, N., and Bauer, S. E.: Improved Attribution of Climate Forcing to Emissions, Science, 326, 716–718, https://doi.org/10.1126/science.1174760, http://science.sciencemag.org/content/326/5953/716, 2009.

Skeie, R., Berntsen, T., Myhre, G., Tanaka, K., Kvalevåg, M., and Hoyle, C.: Anthropogenic radiative forcing time series from pre-industrial times until 2010, Atmos. Chem. Phys., 11, 11 827–11 857, https://doi.org/10.5194/acp-11-11827-2011, https://www.atmos-chem-phys.net/11/11827/2011/, 2011.

Stevens, B.: Rethinking the Lower Bound on Aerosol Radiative Forcing, J. Climate, 28, 4794–4819, https://doi.org/10.1175/JCLI-D-14-00656.1, 2015.

Stevens, B., Sherwood, S. C., Bony, S., and Webb, M. J.: Prospects for narrowing bounds on Earth's equilibrium climate sensitivity, Earth's Future, 4, 512–522, https://doi.org/10.1002/2016EF000376, 2016EF000376, 2016.

Stevenson, D. S., Young, P. J., Naik, V., Lamarque, J.-F., Shindell, D. T., Voulgarakis, A., Skeie, R. B., Dalsoren, S. B., Myhre, G., Berntsen, T. K., Folberth, G. A., Rumbold, S. T., Collins, W. J., MacKenzie, I. A., Doherty, R. M., Zeng, G., van Noije, T. P. C., Strunk, A., Bergmann, D., Cameron-Smith, P., Plummer, D. A., Strode, S. A., Horowitz, L., Lee, Y. H., Szopa, S., Sudo, K., Nagashima, T., Josse, B., Cionni, I., Righi, M., Eyring, V., Conley, A., Bowman, K. W., Wild, O., and Archibald, A.: Tropospheric ozone changes, radiative forcing and attribution to emissions in the Atmospheric Chemistry and Climate Model Intercomparison Project (ACCMIP), Atmos. Chem. Phys., 13, 3063–3085, https://doi.org/10.5194/acp-13-3063-2013, 2013.

Tachiiri, K., Hajima, T., and Kawamiya, M.: Increase of uncertainty in transient climate response to cumulative carbon emissions after stabilization of atmospheric CO2 concentration, Environ. Res. Lett., 10, 125 018, 2015.

Taylor, K. E., Stouffer, R. J., and Meehl, G. A.: An Overview of CMIP5 and the Experiment Design, B. Am. Meteorol. Soc., 93, 485–498, https://doi.org/10.1175/BAMS-D-11-00094.1, 2012.

Thompson, D. W. J., Barnes, E. A., Deser, C., Foust, W. E., and Phillips, A. S.: Quantifying the Role of Internal Climate Variability in Future Climate Trends, J. Climate, 28, 6443–6456, https://doi.org/10.1175/JCLI-D-14-00830.1, 2015.

Toohey, M., Stevens, B., Schmidt, H., and Timmreck, C.: Easy Volcanic Aerosol (EVA v1.0): an idealized forcing generator for climate simulations, Geosci. Model Dev., 9, 4049–4070, https://doi.org/10.5194/gmd-9-4049-2016, https://www.geosci-model-dev.net/9/4049/2016/, 2016.

Twomey, S.: The influence of pollution on the shortwave albedo of clouds, J. Atmos. Sci., 34, 1149–1152, 1977.

Walters, D., Baran, A., Boutle, I., Brooks, M., Earnshaw, P., Edwards, J., Furtado, K., Hill, P., Lock, A., Manners, J., Morcrette, C., Mulcahy, J., Sanchez, C., Smith, C., Stratton, R., Tennant, W., Tomassini, L., Van Weverberg, K., Vosper, S., Willett, M., Browse, J., Bushell, A., Dalvi, M., Essery, R., Gedney, N., Hardiman, S., Johnson, B., Johnson, C., Jones, A., Mann, G., Milton, S., Rumbold, H., Sellar, A., Ujiie, M., Whitall, M., Williams, K., and Zerroukat, M.: The Met Office Unified Model Global Atmosphere 7.0/7.1 and JULES Global Land 7.0 configurations, Geosci. Model Dev. Discuss., 2017, 1–78, https://doi.org/10.5194/gmd-2017-291, https://www.geosci-model-dev-discuss.net/gmd-2017-291/, 2017.

Zhang, H.-M., Huang, B., Lawrimore, J., Menne, M., and Smith, T.: NOAA Global Surface Temperature Dataset (NOAAGlobalTemp), Version 4.0. NOAA National Centers for Environmental Information, https://doi.org/10.7289/V5FN144H, accessed 17 October 2017, 2017.

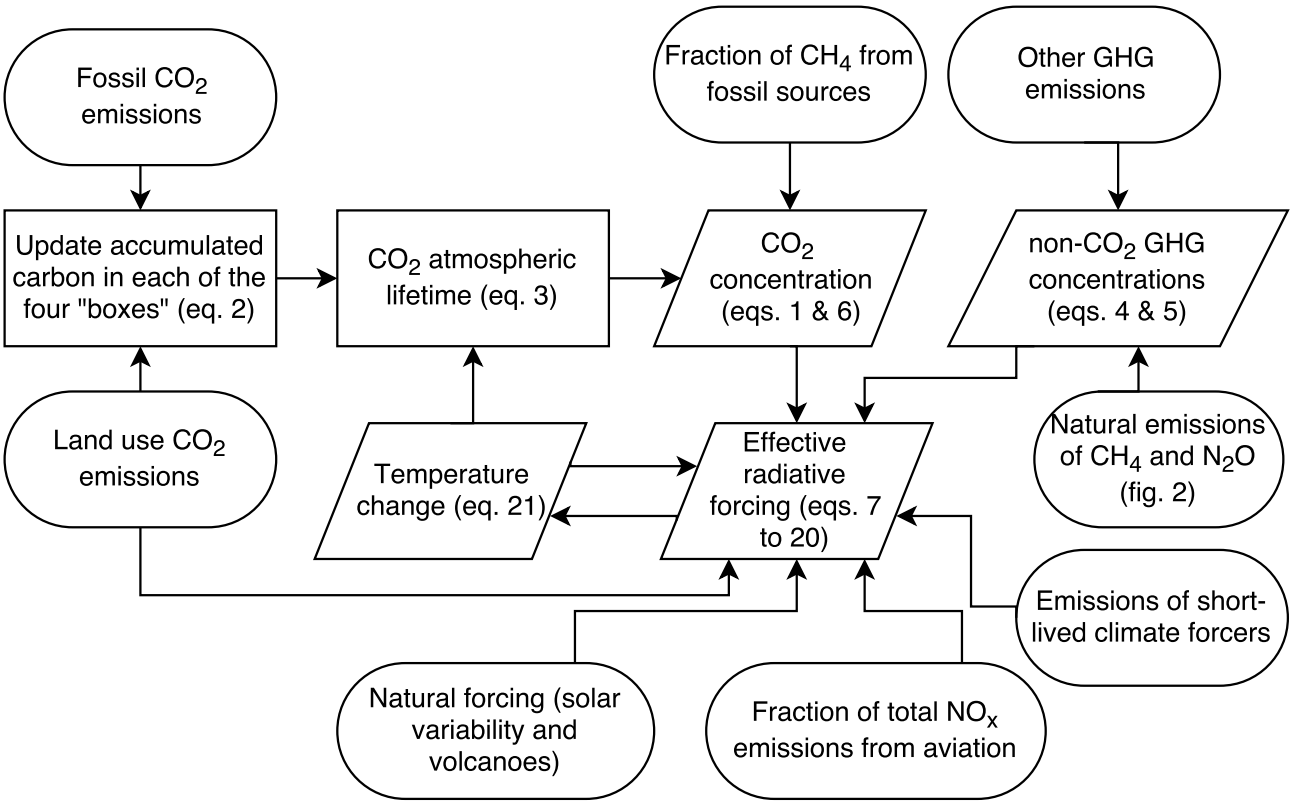

Figure 1. Simplified overview of the FAIR v1.2~~1~~ model.

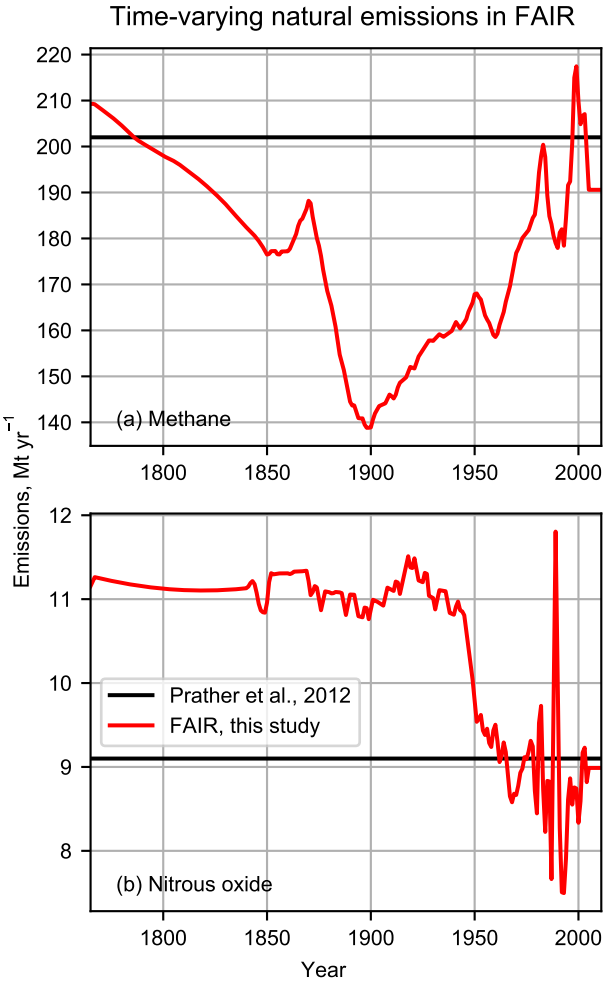

Figure 2. Natural emissions of methane and nitrous oxide used in the FAIR model. Future emissions are fixed at their 2011 values. Also shown are the present-day best estimates of Prather et al. (2012).

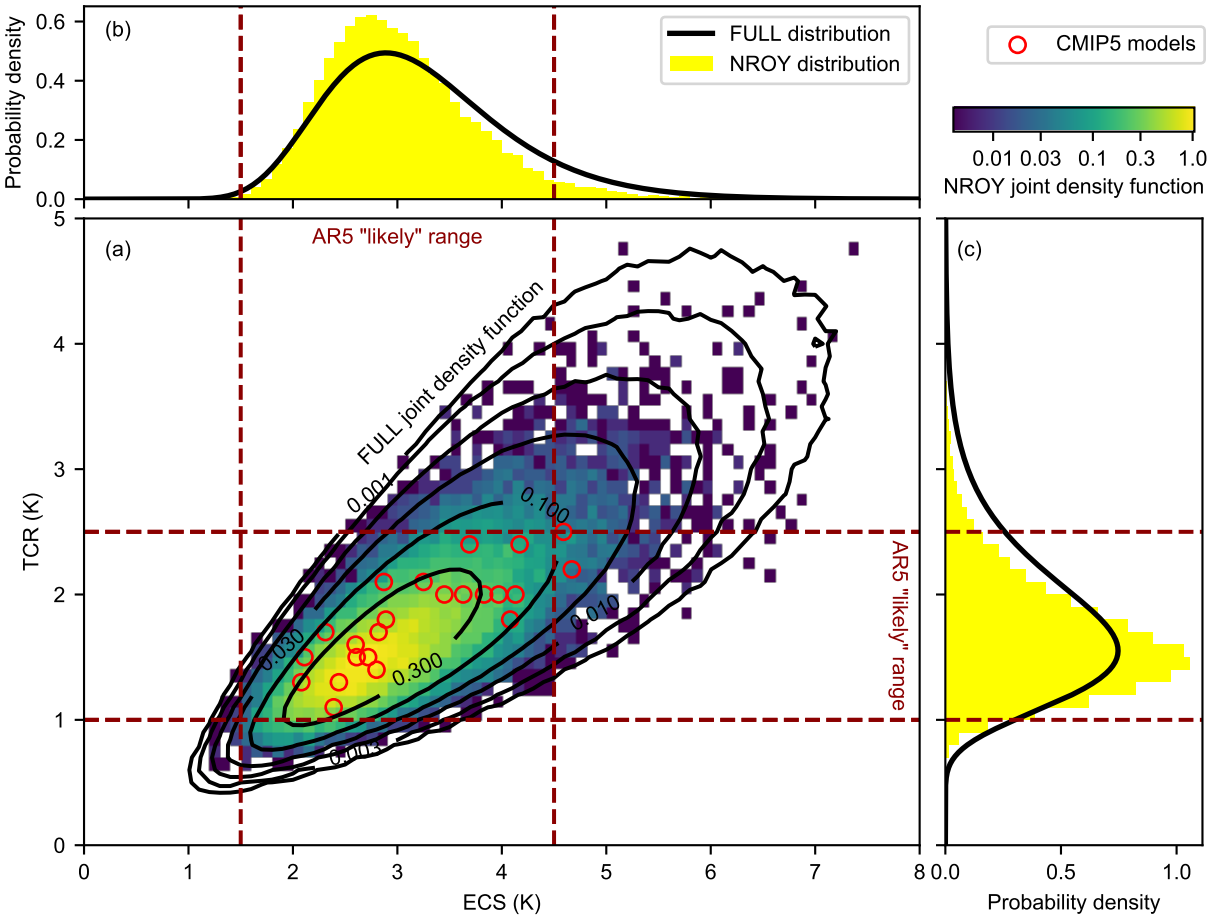

Figure 3. (a) Joint distributions (FULL and NROY) of ECS and TCR. (b) Marginal distributions of ECS. (c) Marginal distributions of TCR. In (a), the FULL distribution is shown with open black contours and the NROY distribution with coloured squares. Probability density is plotted on a log scale. In (b) and (c), the FULL distribution is shown as a black curve and the NROY distribution with yellow histogram bars, both plotted on a linear scale. The NROY distributions contains only those ensemble members which agree with the C&W observed historical temperatures. CMIP5 models are depicted with red circles.

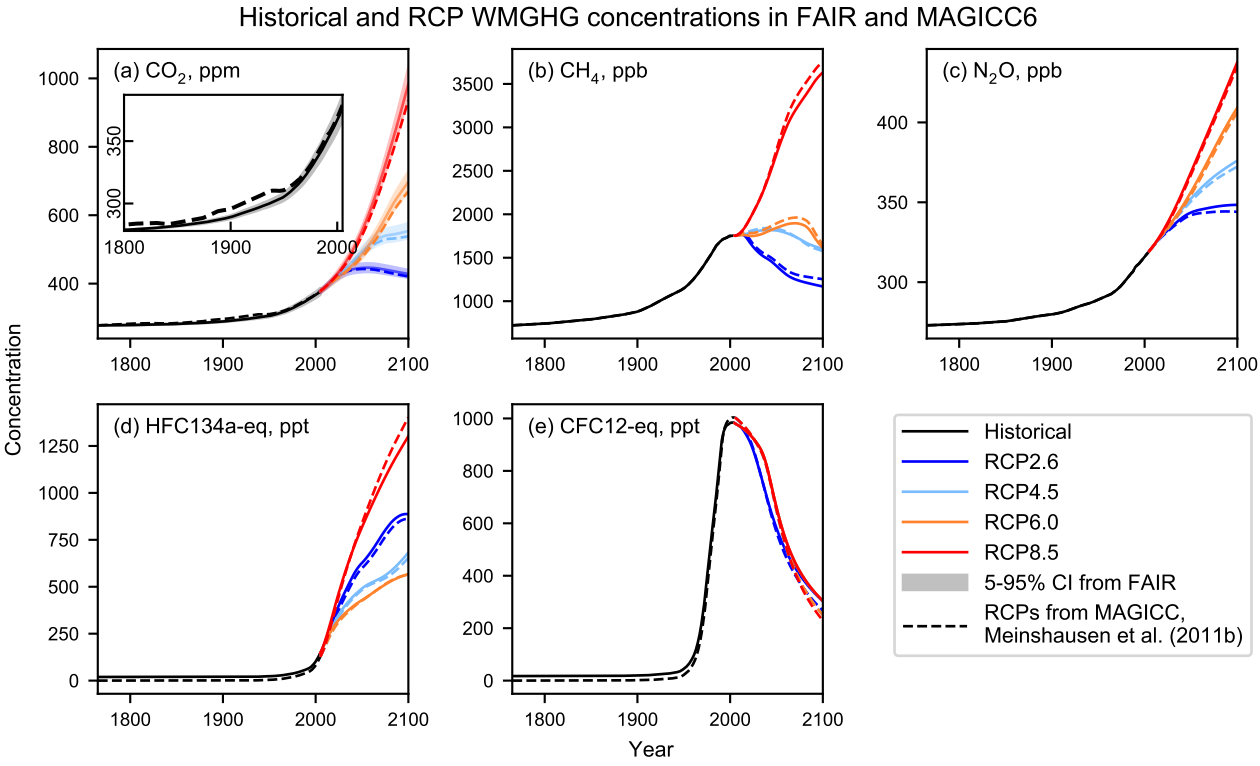

Figure 4. Comparison of the historical and RCP greenhouse gas concentrations in FAIR (heavy solid lines) with 5-95% confidence intervals (shading) for CO_2. Dashed lines show the concentrations from MAGICC6 (Meinshausen et al., 2011b). For CFC12-eq, the RCP4.5 and RCP6.0 lines lie underneath the RCP8.5 line.

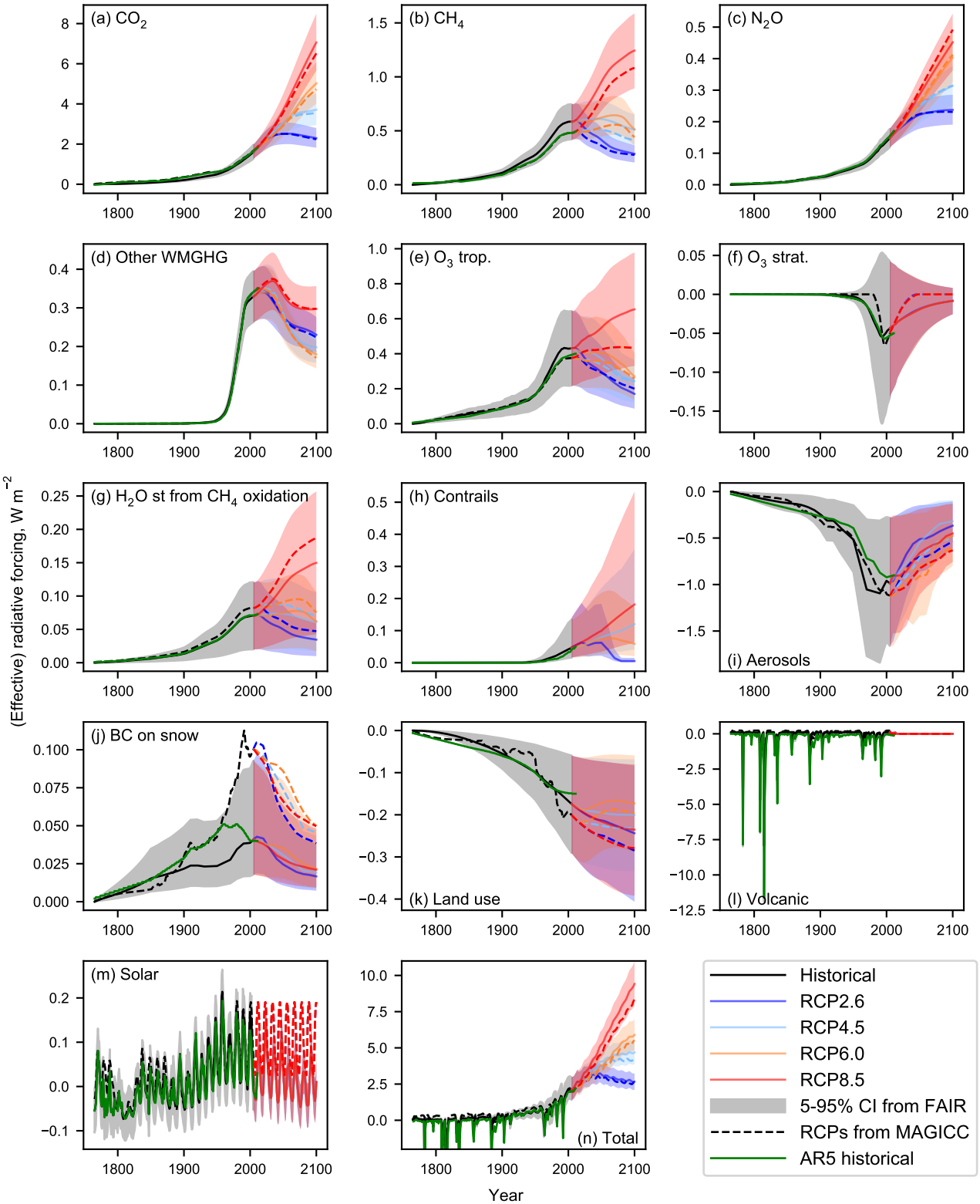

Figure 5. Comparison of the radiative forcing from RCP2.6, RCP4.5, RCP6.0 and RCP8.5 derived from 13 separate components (subplots a–m), along with the total radiative forcing (subplot n). ERF from FAIR (solid lines) with 5-95% confidence intervals (shading), RF from MAGICC6 (dashed lines, Meinshausen et al. (2011b)) and RF from AR5 Annex II for 1850–2011 (green solid lines, IPCC (2013)).

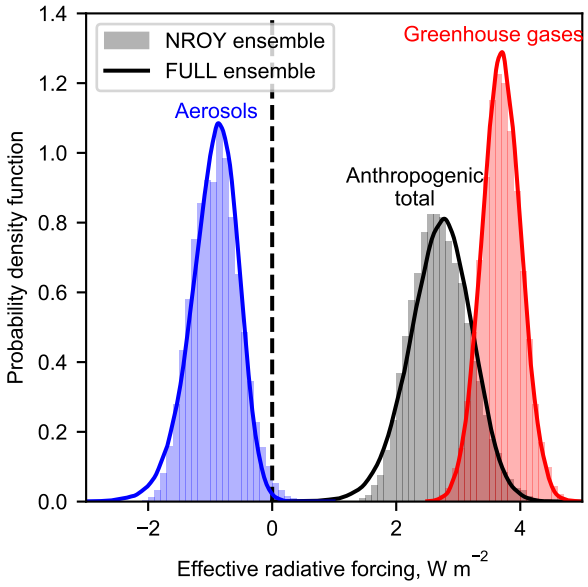

Figure 6. ERF from aerosols (blue), greenhouse gases (red) and total anthropogenic (black) for present-day (2017, based on RCP8.5) runs from FAIR constrained to observed temperature change (NROY; histograms) and from prior distributions (FULL; curves); compare Myhre et al. (2013b, Figure 8.16). Greenhouse gas forcing includes contributions from ozone and stratospheric water vapour from methane. Anthropogenic total is the sum of greenhouse gas, aerosol, contrails, BC on snow and land use change. The latter three distributions are not shown separately.

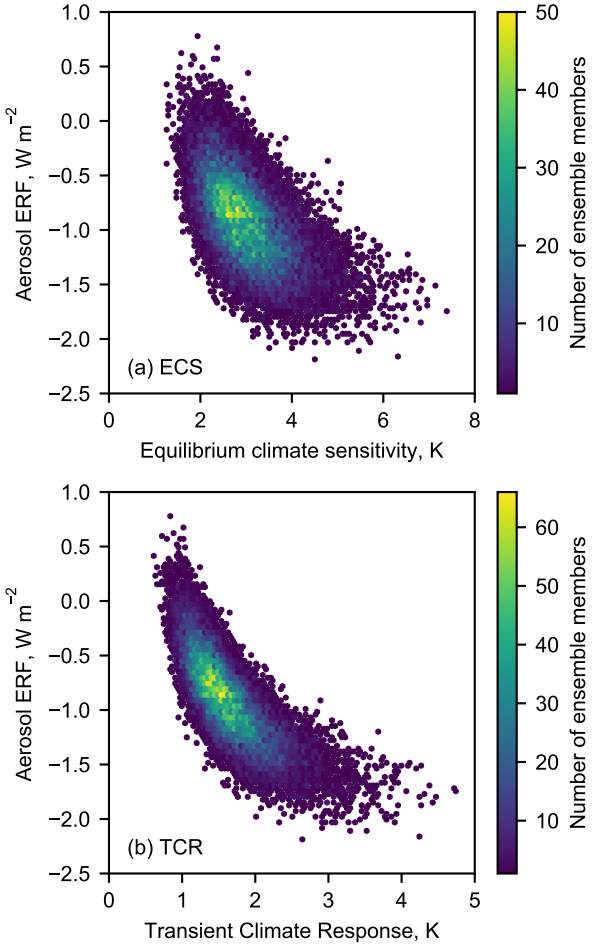

Figure 7. Relationship between (a) ECS and aerosol ERF; (b) TCR and aerosol ERF for the NROY ensemble. Aerosol ERF is shown for 2017 under the RCP8.5 scenario.

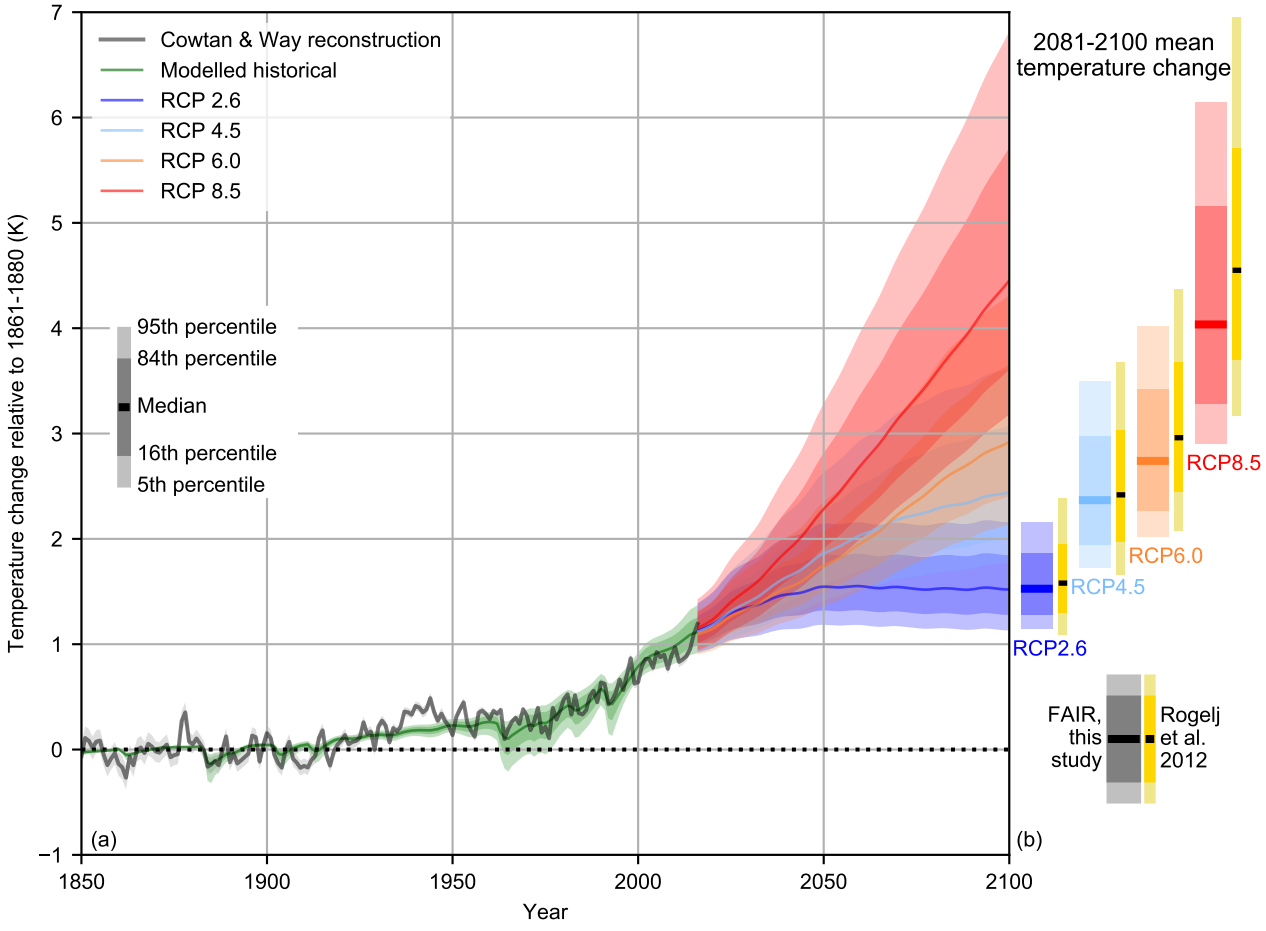

Figure 8. (a) Historical constrained modelled temperature and future probabilistic temperature scenarios from FAIR driven by emissions and forcing from the RCPs for 1850–2100 expressed as temperature change since 1861–1880. Also shown is observed temperature from C&W. (b) Comparison of 2081–2100 mean temperature from FAIR compared to the emission-driven ensemble from MAGICC6 (Rogelj et al., 2012).

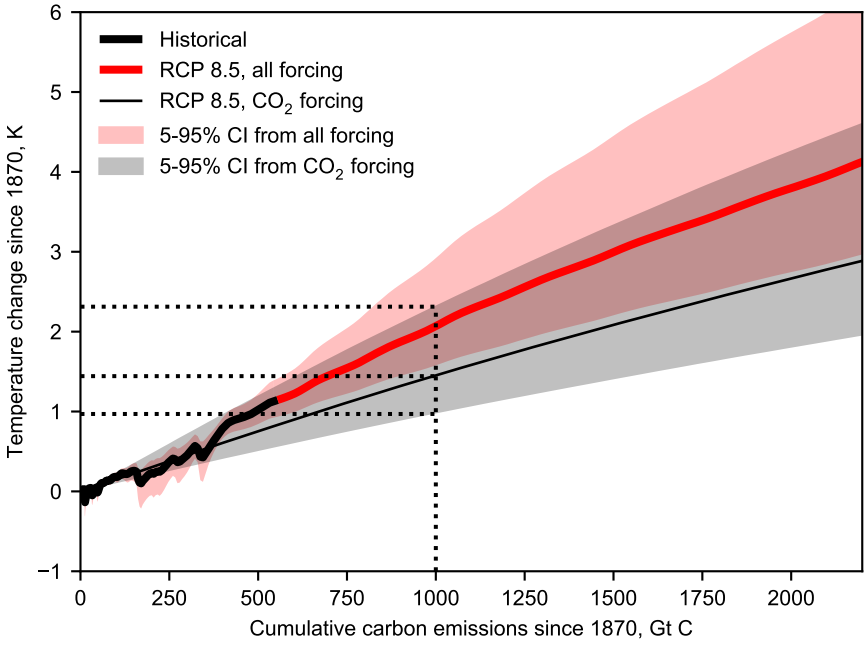

Figure 9. Transient climate response to CO_2 emissions (TCRE) for FAIR based on RCP8.5 for all forcing (red) and for CO_2-only forcing (black). ~~The 90% uncertainty range for CO_2 forcing is not shown for historical temperature change as the ratio F_{CO_2}/F is very sensitive to periods where volcanic forcing is dominant.~~

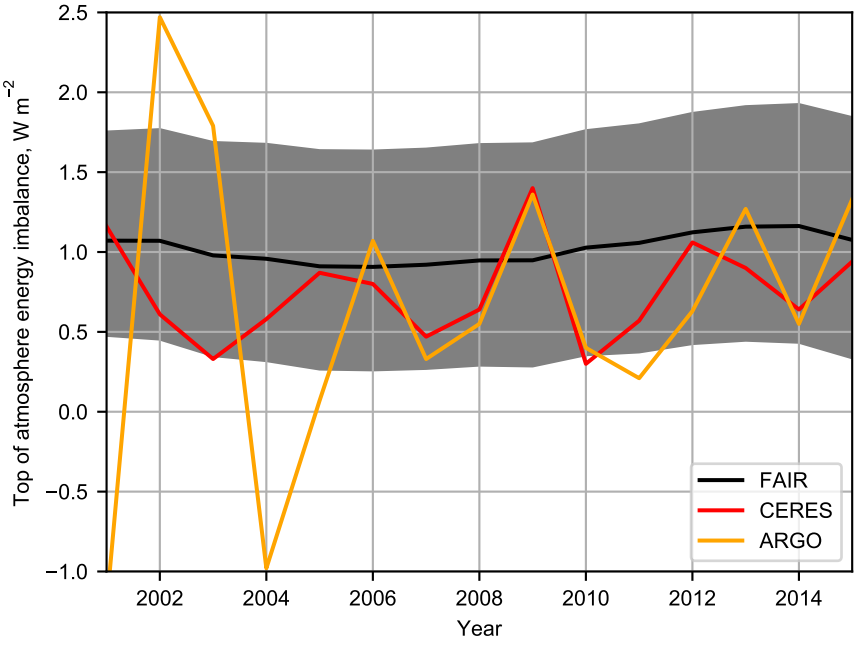

Figure 10. Comparison of earth's energy imbalance N to observations from Argo and CERES, from Johnson et al. (2016).

Table 1. Emissions time series input used in FAIR, based on the RCP emissions datasets in Meinshausen et al. (2011b).

Index	Species	Unit	Remark
0	Year	Year	Important for running RCP scenarios as some treatments differ before 1850
1	CO_2 fossil	Gt C yr^{-1}	
2	CO_2 land-use	Gt C yr^{-1}	
3	CH_4	Mt yr^{-1}	Only anthropogenic emissions
4	N_2O	Mt N_2 yr^{-1}	Only anthropogenic emissions, expressed as N_2 equivalent mass
5	SOx	Mt S yr^{-1}	Only anthropogenic emissions
6	CO	Mt yr^{-1}	Only anthropogenic emissions
7	NMVOC	Mt yr^{-1}	Only anthropogenic emissions
8	NOx	Mt N yr^{-1}	Only anthropogenic emissions
9	BC	Mt yr^{-1}	Only anthropogenic emissions
10	OC	Mt yr^{-1}	Only anthropogenic emissions
11	NH_3	Mt yr^{-1}	Only anthropogenic emissions
12	CF_4	kt yr^{-1}	Natural emissions should be included
13	C_2F_6	kt yr^{-1}	
14	C_6F_{14}	kt yr^{-1}	
15	HFC23	kt yr^{-1}	
16	HFC32	kt yr^{-1}	
17	HFC43-10	kt yr^{-1}	
18	HFC125	kt yr^{-1}	
19	HFC134a	kt yr^{-1}	
20	HFC143a	kt yr^{-1}	
21	HFC227ea	kt yr^{-1}	
22	HFC245fa	kt yr^{-1}	
23	SF_6	kt yr^{-1}	
24	CFC11	kt yr^{-1}	
25	CFC12	kt yr^{-1}	
26	CFC113	kt yr^{-1}	
27	CFC114	kt yr^{-1}	
28	CFC115	kt yr^{-1}	
29	CCl_4	kt yr^{-1}	
30	Methyl chloroform	kt yr^{-1}	
31	HCFC22	kt yr^{-1}	
32	HCFC141b	kt yr^{-1}	
33	HCFC142b	kt yr^{-1}	
34	Halon 1211	kt yr^{-1}	
35	Halon 1202	kt yr^{-1}	
36	Halon 1301	kt yr^{-1}	
37	Halon 2401	kt yr^{-1}	
38	CH_3Br	kt yr^{-1}	Natural emissions should be included
39	CH_3Cl	kt yr^{-1}	Natural emissions should be included

Table 2. The set of greenhouse gases used in FAIR. With the exception of methane lifetime, radiative efficiencies and lifetimes are from AR5 (Myhre et al., 2013b, table 8.A.1). For ozone-depleting substances, the fractional release coefficients r_i (Daniel and Velders, 2011) and the number of chlorine and bromine atoms are also given, for calculation of equivalent effective stratospheric chlorine (eq. (14)).

Index	Gas	Molecular weight w_f (g mol^{-1})	Radiative efficiency η (W m^{-2} ppb^{-1})	Lifetime τ (yr)	r_i	n_{Cl}	n_{Br}
			Major gases				
0	CO_2	44.01	N/A	Variable			
1	CH_4	16.04	N/A	9.3			
2	N_2O	44.01	N/A	121			
			Kyoto Protocol gases				
3	CF_4	88.00	0.09	50000			
4	C_2F_6	138.01	0.25	10000			
5	C_6F_{14}	338.04	0.44	3100			
6	HFC23	70.01	0.18	222			
7	HFC32	52.02	0.11	5.2			
8	HFC43-10	252.06	0.42	16.1			
9	HFC125	120.02	0.23	28.2			
10	HFC134a	102.03	0.16	13.4			
11	HFC143a	84.04	0.16	47.1			
12	HFC227ea	170.03	0.26	38.9			
13	HFC245fa	134.05	0.24	7.7			
14	SF_6	146.06	0.57	3200			
			Ozone depleting substances				
15	CFC11	137.37	0.26	45	0.47	3	0
16	CFC12	120.91	0.32	100	0.23	2	0
17	CFC113	187.38	0.30	85	0.29	3	0
18	CFC114	170.92	0.31	190	0.12	2	0
19	CFC115	154.47	0.20	1020	0.04	1	0
20	CCl_4	153.81	0.17	26	0.56	4	0
21	Methyl chloroform	133.40	0.07	5	0.67	3	0
22	HCFC22	86.47	0.21	11.9	0.13	1	0
23	HCFC141b	116.94	0.16	9.2	0.34	2	0
24	HCFC142b	100.49	0.19	17.2	0.17	1	0
25	Halon 1211	165.36	0.29	16.0	0.62	1	1
26	Halon 1202	209.82	0.27	2.9	0.62	0	2
27	Halon 1301	148.91	0.30	65	0.28	0	1
28	Halon 2401	259.82	0.30	20	0.65	0	2
29	CH_3Br	94.94	0.004	0.8	0.60	0	1
30	CH_3Cl	50.49	0.01	1	0.44	1	0

Table 3. The 13 separate forcing groups considered in FAIR v1.2~~1~~ in the calculation of effective radiative forcing. The ERF uncertainty represents the 5–95% range and is used in the generation of the large ensemble (section 3). ERF uncertainties from Myhre et al. (2013b) are used except for CH_4 where we use the Myhre et al. (2013b) estimate inflated by the additional uncertainty in the new methane forcing relationship in Etminan et al. (2016), which also affects the uncertainty in stratospheric water vapour oxidation from methane.

Index	Forcing agent	Depends on	ERF uncertainty
0	CO_2	CO_2 emissions; CH_4 fossil fraction; cumulative C emissions; total temperature change	$\pm 20\%$
1	CH_4	CH_4 emissions	$\pm 28\%$
2	N_2O	N_2O emissions	$\pm 20\%$
3	Other greenhouse gases	Emissions of other greenhouse gases	$\pm 20\%$
4	Tropospheric ozone	Emissions of CH_4 and short-lived climate forcers	$\pm 50\%$
5	Stratospheric ozone	Concentrations of ozone depleting substances (subset of minor greenhouse gases)	$\pm 200\%$
6	Stratospheric water vapour	CH_4 ERF	$\pm 72\%$
7	Contrails	Aviation NOx fraction; total NOx emitted	-66 to $+191\%$
8	Aerosols	Emissions of short-lived climate forcers	-89 to $+111\%$
9	Black carbon on snow	Emissions of black carbon	-56 to $+128\%$
10	Land use change	Cumulative emissions of land-use related CO_2	$\pm 167\%$
11	Volcanic	Externally supplied forcing from volcanoes	$\pm 50\%$
12	Solar	Externally supplied forcing from solar variability	± 0.05 W m^{-2}

Table 4. Contribution to tropospheric ozone ERF from each precursor. Pre-industrial emissions from Skeie et al. (2011), pre-industrial CH_4 from Meinshausen et al. (2011b), 1850 and 2000 emissions from Lamarque et al. (2010) and 2000 minus 1850 ERF from Stevenson et al. (2013).

		Ozone forcing efficiency β_i (eq. (11))		
Species	ERF in 2000 (W m^{-2})	Pre-1850	Post-1850	Pre-industrial value
CH_4	0.178	1.73×10^{-4}	1.73×10^{-4} W m^{-2} ppb^{-1}	722 ppb
CO	0.076	4.76×10^{-5}	8.51×10^{-5} W m^{-2} (Mt yr^{-1})$^{-1}$	170 Mt CO yr^{-1}
NMVOC	0.044	1.88×10^{-4}	2.25×10^{-4} W m^{-2} (Mt yr^{-1})$^{-1}$	5 Mt NMVOC yr^{-1}
NOx	0.125	5.72×10^{-4}	9.08×10^{-4} W m^{-2} (Mt yr^{-1})$^{-1}$	2 Mt N yr^{-1}

Table 5. Contribution to ERFari from each aerosol precursor species and contribution to 2011 ERFari.

Species	ERFari in 2011 (W m^{-2})	Radiative efficiency (10^{-3} W m^{-2} (Mt yr^{-1})$^{-1}$)
SOx	-0.484	-9.69 (Mt S)
BC	$+0.497$	$+62.2$
OC	-0.184	-5.20
NH_3	-0.063	-1.42
NOx	-0.067	-1.70 (Mt N)
SOA	-0.150	-0.692

Table 6. Median and 5–95% credible intervals for effective radiative forcing from greenhouse gases, aerosols and anthropogenic total from the FULL and NROY FAIR ensembles in 2017. Anthropogenic total contains contributions from contrails, BC on snow and land use change and therefore is not equal to the sum of greenhouse gas and aerosol forcing. Compare fig. 6.

	Radiative forcing (W m^{-2})	
Forcing type	Before temperature constraint (FULL)	After temperature constraint (NROY)
Greenhouse gases	3.69 (3.18 to 4.21)	3.69 (3.17 to 4.24)
Aerosols	-0.91 (-1.63 to -0.37)	-0.90 (-1.51 to -0.26)
Anthropogenic total	2.73 (1.85 to 3.50)	2.70 (1.98 to 3.54)

Table 7. Sensitivity in the ECS, TCR, TCRE to variations in the underlying assumptions in the FAIR large ensemble. For the sensitivity experiments the section number in the manuscript describing the change is given. The Accepted column details the proportion of the 100,000 member FULL ensemble that satisfied the specified temperature constraint.

Variation (section)	Accepted	ECS (K)			TCR (K)			TCRE (K (Eg C)$^{-1}$)		
		5%	50%	95%	5%	50%	95%	5%	50%	95%
C&W temperature constraint (NROY)	25.0%	2.04	2.93	4.32	1.07	1.59	2.50	0.97	1.44	2.31
C&W with alternative ECS/TCR prior (5.1)	21.1%	1.60	2.76	4.92	1.00	1.64	2.76	0.90	1.45	2.61
C&W with $F_{2\times} = 3.44$ W m^{-2} (5.2)	23.8%	2.02	2.92	4.32	1.05	1.58	2.50	0.93	1.40	2.32
HadCRUT4 temperature constraint (5.3)	25.8%	2.00	2.89	4.30	1.04	1.56	2.47	0.94	1.42	2.30
GISTEMP temperature constraint (5.3)	31.7%	2.06	2.96	4.35	1.08	1.61	2.53	0.98	1.46	2.35
Berkeley Earth temperature constraint (5.3)	21.9%	2.12	3.03	4.42	1.14	1.66	2.58	1.03	1.51	2.39
NOAA temperature constraint (5.3)	34.2%	2.01	2.91	4.32	1.04	1.57	2.50	0.94	1.43	2.30
No temperature constraint (FULL)	100%	2.00	3.11	4.86	1.01	1.73	2.96	0.91	1.58	2.78

Table 8. Sensitivity in the effective radiative forcing to variations in the underlying assumptions in the FAIR large ensemble.

Variation	Effective radiative forcing in 2100, W m^{-2}											
	RCP 2.6			RCP 4.5			RCP 6.0			RCP 8.5		
	5%	50%	95%	5%	50%	95%	5%	50%	95%	5%	50%	95%
C&W temperature constraint (NROY)	2.12	2.67	3.25	3.89	4.69	5.53	4.86	5.90	6.98	7.93	9.42	10.95
C&W with alternative ECS/TCR prior	2.10	2.66	3.26	3.88	4.69	5.52	4.84	5.90	6.97	7.92	9.42	10.94
C&W with $F_{2\times} = 3.44$ W m^{-2}	1.98	2.49	3.04	3.67	4.42	5.20	4.56	5.53	6.54	7.51	8.90	10.34
HadCRUT4 temperature constraint	2.10	2.64	3.22	3.87	4.66	5.49	4.83	5.86	6.93	7.90	9.37	10.90
GISTEMP temperature constraint	2.13	2.68	3.27	3.90	4.70	5.56	4.87	5.92	7.01	7.94	9.44	10.98
Berkeley Earth temperature constraint	2.17	2.72	3.31	3.94	4.75	5.61	4.92	5.98	7.08	8.00	9.52	11.06
NOAA temperature constraint	2.10	2.65	3.24	3.87	4.67	5.52	4.83	5.88	6.96	7.91	9.39	10.93
No temperature constraint (FULL)	1.92	2.67	3.41	3.73	4.69	5.70	4.63	5.89	7.19	7.73	9.41	11.17

Table 9. Sensitivity in the 2100 temperature change in RCP scenarios to variations in the underlying assumptions in the FAIR large ensemble.

Variation	temperature change in 2100 from 1861–1880 mean, K											
	RCP 2.6			RCP 4.5			RCP 6.0			RCP 8.5		
	5%	50%	95%	5%	50%	95%	5%	50%	95%	5%	50%	95%
C&W temperature constraint (NROY)	1.13	1.52	2.16	1.77	2.44	3.62	2.14	2.92	4.32	3.18	4.45	6.82
C&W with alternative ECS/TCR prior	0.98	1.48	2.37	1.56	2.43	4.06	1.91	2.94	4.80	2.88	4.52	7.61
C&W with $F_{2\times} = 3.44$ W m^{-2}	1.13	1.53	2.18	1.78	2.47	3.68	2.14	2.93	4.37	3.20	4.51	6.95
HadCRUT4 temperature constraint	1.09	1.48	2.12	1.71	2.39	3.58	2.07	2.85	4.25	3.08	4.35	6.73
GISTEMP temperature constraint	1.14	1.55	2.20	1.79	2.49	3.68	2.16	2.98	4.39	3.22	4.54	6.92
Berkeley Earth temperature constraint	1.22	1.62	2.27	1.92	2.58	3.78	2.32	3.09	4.51	3.43	4.70	7.09
NOAA temperature constraint	1.09	1.50	2.16	1.71	2.42	3.61	2.06	2.89	4.31	3.08	4.41	6.80
No temperature constraint (FULL)	0.92	1.63	2.90	1.54	2.65	4.66	1.82	3.17	5.63	2.80	4.88	8.62